THE IMPACT OF POPULATION HETEROGENEITIES AND DISEASE INTERVENTIONS ON HERD IMMUNITY:

A CASE STUDY OF THE COVID-19 PANDEMIC IN ONTARIO

MARIA GENEVA ROSELLE LIWAG

A THESIS SUBMITTED TO THE FACULTY OF GRADUATE STUDIES
IN PARTIAL FULFILMENT OF THE REQUIREMENTS
FOR THE DEGREE OF
MASTER OF SCIENCE

GRADUATE PROGRAM IN DEPARTMENT OF MATHEMATICS AND STATISTICS
YORK UNIVERSITY
TORONTO, ONTARIO

OCTOBER 2022

Abstract

In epidemiology, herd immunity refers to the population level of immunity required to prevent a large disease outbreak or extinguish an outbreak. Previous work shows that herd immunity level in models with homogeneously mixing assumptions and without demographic structures may be different from that in heterogeneous models. With the COVID-19 pandemic in Ontario as a case study, a comprehensive deterministic mathematical model of disease spread with age and contact pattern variations was developed to examine the required herd immunity for different variants and compare with the theoretical values obtained using homogeneous assumptions. The effects of non-pharmaceutical (testing/isolation of silent infections) interventions and vaccination on epidemic progression and herd immunity were investigated. It was found that with the inclusion of age and contact pattern structures, the resulting herd immunity level required to end an epidemic under the assumptions of long-term protection (i.e., without re-infection) is lower than theoretical values, even for more transmissible variants. Moreover, while waning immunity and eventual re-infection results in an oscillation in herd immunity levels in the population, subsequent epidemic peaks are less amplified, suggesting that even with increased variant transmissibility, infections of any variant allow for the rise of immunity in the population, leading to an endemic state.

Para kina Ma, Dad, Noy at Lola –

aking mga pinakamamahal.

Acknowledgements

I would like to extend my sincerest gratitude and appreciation to the following people, without whom this thesis will forever remain an unfinished draft:

To my supervisor, Prof. Seyed Moghadas, for his unwavering guidance and support, from the first advising meeting back in July 2020, through the first year of coursework, the second year of thesis work, all the way to the end. I've learned a lot over these past two years as a member of the ABM-Lab, and completing this thesis would not be possible without your help and immense patience.

To my supervisory committee: Prof. Neal Madras, Prof. Jianhong Wu, Prof. Dasantila Golemi-Kotra, and Dr. Affan Shoukat, for their comments and suggestions to improve on this thesis, from the seminar presentations to the defence.

To my ABM-Lab *kuya* and *ates*: Thomas Vilches, Ellie Abdollahi, and Mehreen Tariq, for reminding me that I don't have to go through academia life alone, and that it's never wrong to ask for help from those who've made it through before.

To Aziza Kajan and the Graduate Student Wellness Services at York University, for providing me a safe space to unload my anxieties, for guiding me through resolving them step by step, and for showing me that there's always calm amidst the chaos.

To the York Math graduate students and post-docs, whom I've either taken classes with or met at social events after one year of "Zoom University", for making the graduate school experience memorable. It was a pleasure working with such wonderful and interesting people.

To my friends from undergrad who have kept in touch during my time at York, especially Jeff Carlson, Johnny Nguyen, and Jérémy Belliveau, for keeping me sane in their own pretty little ways, from graduate school struggle stories to cute animal videos on Instagram.

To the *anti-momo* Brandon Davila, for keeping this *half-momo* grounded from 584 kilometres away with food rants, Spotify cry sessions, TikTok backlog, and sane advice that never miss.

To Grégoire Ranson, for being the best support this *smol bean* could have during the final push towards defence and graduation. What started out as coffee and company in the Scott Library graduate room turned into a connection rooted in steadfast kindness and mutual understanding, and I couldn't ask for a better academia colleague, friend, and partner. Thank you for being my plot twist, and I look forward to more surprises.

To Laika Ancog and Pauline Bautista, for being my cheerleaders and fail-proof support system from 12 time zones away. Thank you for letting me send countless text and video rants (academic, romantic, and existential), and for sending back takes that always make perfect sense. Here's to more than a decade of friendship, and I miss you so.

To the *titos* and *titas* of Manila, the San Diego gang, and the Dalisay-Mariño clan, for their continuous love and support, and for sending me strength from wherever they may be.

And finally, to the Managers: my parents Gerald and Rosalia Liwag, my brother Marcus Liwag, and my *lola* Maria Mariño, for supporting my path to graduate studies in a completely different field, for celebrating with me even the smallest of wins, for being immensely understanding and patient at my lowest points, and for continuing to believe in me even when I stopped believing in myself. As long as I've made you proud, I can say my job here is done. I've got it all. I'm happy. I love you.

Contents

List of Tables

List of Figures

Chapter 1

Introduction

1.1 The novel coronavirus disease (COVID-19)

Since the first identified case in Hubei Province, China in November 2019 [1], the novel coronavirus disease (COVID-19) has caused significant public health toll in terms of infections, hospitalizations and deaths worldwide, with over 500 million cases and 6.3 million deaths reported [2].

As of September 24, 2022, there have been over 4 million cases of COVID-19 and more than 45,000 deaths in Canada, with the majority of cases occurring in Ontario (1,444,227 cases and 14,312 deaths) and Québec (1,196,164 cases and 16,680 deaths) [3]. In the absence of pharmaceutical preventive measures such as vaccination in the early stages of the pandemic, countries worldwide used numerous non-pharmaceutical interventions in order to quell the spread of the disease. On a national or provincial scale, such interventions included border closures and lockdowns of various strengths [4]. Meanwhile, measures that were mandated by public health agencies for individuals to follow included physical distancing and self-isolation upon experiencing symptoms of COVID-19 [4, 5].

Over the course of the pandemic, several variants of concern (VOCs) of SARS-CoV-2

have emerged identified [6], with distinct and varying degree of transmission, disease severity, and lethality compared to the original strain (Wuhan-I). The Alpha (B.1.1.7) variant, first identified in the United Kingdom in September 2020 [7], raised concerns due to its increased severity and mortality. Relative to the original variant, there were reported 43–90% increase in transmissibility [8], and 61% increase in risk of death among those infected with the Alpha variant [9]. Later, in April 2021, a new variant of concern, named Delta (B.1.617.2), emerged. This variant was first documented in COVID-19 patients in India [7]. Similar to the Alpha variant, Delta exhibited an increased transmissibility, with studies reporting an even greater (76—117%) increase relative to the original strain [10]. Moreover, analysis of hospital admission in Ontario found that the Delta variant was associated with 108% increase in the risk of hospitalization and 132% risk of death due to severe disease [11].

The most recent variant of concern, Omicron (B.1.1.529), presumably emerged in South Africa in November 2021, but was also detected in multiple countries around the same time [7]. While Omicron exhibited far greater transmissibility than the previous variants, studies in England and South Africa found that it was associated with a lower risk of severe disease and hospitalisation [12, 13]. However, it was rapidly discovered that the Omicron variant carries mutations that can escape neutralizing antibodies generated by prior infection or vaccination, causing a significant number of reinfections and the largest pandemic wave in affected countries [14, 15]. Since its emergence, numerous subvariants of Omicron have evolved with greater degree of immune escape, further hindering efforts to control COVID-19 pandemic based on the existing levels of population immunity generated by natural infections or currently available vaccines.

1.2   Motivation and objectives

In mathematical epidemiology, herd immunity $\mathcal{H}_c$ is defined as the population level of immunity required to prevent a large disease outbreak or extinguish an ongoing outbreak [16]. In simple, homogeneous models of disease spread in the population [17, 18], there is a well-established relationship between the herd immunity and the basic reproduction number $\mathcal{R}_0$, defined as the average number of new infections caused by an infected individual in an entirely susceptible population [19]. This relationship, given by $\mathcal{H}_c = 1 - 1/\mathcal{R}_0$ [16], determines the type and intensity of interventions required to curb a disease epidemic. For example, in the context of vaccination with 100% protection against infection, if vaccines are distributed uniformly and a p-proportion of the population is vaccinated, the reproduction number is expected to reduce to $(1 - p)\mathcal{R}_0$ [20], which in turn would affect $\mathcal{H}_c$. Thus, in classical models, reducing $\mathcal{R}_0$ to below 1 leads to epidemic control [17], suggesting that the required level of herd immunity has reached.

In realistic settings, however, no population mixes homogeneously and no vaccine can provide full protection to all vaccinated individuals due to host factors and vaccine properties [21–23]. Thus, the required level of herd immunity or the proportion of population to be vaccinated for disease control may differ from the theoretical assertion by models under the assumption of homogeneous mixing [24]. Since, in most cases, recovery from infection increases herd immunity in the population, understanding the required threshold of population immunity for disease control is critically important for the application of other intervention measures in the absence of vaccination.

Early studies on the effect of heterogeneity on herd immunity, specifically for the COVID-19 pandemic, involved implementing age stratification and contact variations among these age groups [24, 25]. On top of the different contact rates per age group, social activity of individuals were also varied by scaling these contact rates to represent low, moderate, or

high activity [24]. As lockdown measures were the primary non-pharmaceutical intervention during the early stages of the pandemic, the effect of imposing lockdown with varying strength and duration onto the population was explored [24]. Similar to the social activity, lockdown strength was implemented by scaling down contact rates across all age groups, with lower contact rates resulting from greater lockdown strength. It was found that with these variations in age and contact structures, the herd immunity level required to prevent a second wave of COVID-19 infections was 43% for $\mathcal{R}_0 = 2.5$ [24] and 53% for $\mathcal{R}_0 = 2.3$ [25], lower than the value obtained using homogeneous assumptions (60% for $\mathcal{R}_0 = 2.5$, 56.5% for $\mathcal{R}_0 = 2.3$). However, this study assumed that the the scaling of contact rates for both social activity and lockdown strength act proportionally for all individuals regardless of age group or disease stage [24]; it did not consider that infected individuals can be identified and isolated at any stage of infection, leading to a reduction in contacts during the course of isolation. Moreover, the model used in this study did not categorise infectious individuals as either in the asymptomatic or symptomatic stages; this can influence epidemic dynamics, and thus herd immunity, due to differences in transmissibility of infections [26–29].

In this thesis, I propose a modelling framework for disease spread to account for heterogeneities in the population by considering two main factors of age and contact patterns among individuals. Using this framework, first I will show how the herd immunity level is affected by these factors and quantify its divergence from the theoretical expression, which is based on simple homogeneous assumptions. Then, I will implement interventions to evaluate how control measures affect the level of herd immunity. For diseases that may be subject to multiple epidemic waves, such as COVID-19 pandemic, I will investigate how the intermittent intensity of interventions can influence the ultimate level of herd immunity that may depend on the prevalence of infection at the time of relaxing measures. Finally, I will integrate an imperfect vaccination into the model to explore the heterogeneous effects of vaccine protection on the creation of herd immunity in the context of other intervention measures.

Chapter 2

Background

2.1 Timelines of COVID-19 in Ontario

The first case of COVID-19 in Ontario was recorded on January 25, 2020, from a patient who arrived in Canada from Wuhan, China [30]. Case counts started to rise, and on March 11, 2020, the first death caused by COVID-19 was confirmed: a 77-year-old man with prior close contact with an infected person [31]. The provincial government declared a state of emergency on March 17, 2020, starting the mandatory closure of schools and non-essential workplaces, and effectively putting the province in a lockdown [32]. Majority of the cases recorded in this early stage came from long-term care homes (LTCH), with the first outbreak being declared on March 20, 2020 in Bobcaygeon, Ontario. Within 20 days, there were 29 resident deaths tallied [33]. Towards the end of the first wave in July 2020, there were close to 6000 cases and 390 outbreaks in LTCHs in Ontario, with 32.6% of those cases resulting to deaths [34].

Case counts in Ontario began to rise again as the fall season approached, and by September 28, 2020, a new high of 700 new cases per day were reported, which was more than the previous high of 640 cases recorded during the first wave [35]. Still, likely many more cases

5

were not documented due to limited testing, and lack of clinical symptoms for may infected individuals. While there was still concern for the elderly population, it was noted that 60% of those new cases were among individuals under 40 years of age [35]. New cases continued to rise during the second wave with previous single-day new case records being broken almost every day. At the peak of the second wave on January 7, 2021, 3,519 new cases were recorded, despite the COVID-19 vaccines already being available for distribution to key vulnerable populations [36].

Apart from the increasing number of new cases, the emergence of new COVID-19 variants of concern (VOCs) further exacerbated the effect of the pandemic on the province. The first known case of the Alpha variant in Ontario was identified on December 26, 2020, from a couple in Durham, Ontario with no known history of international travel or exposure to infected individuals [37], suggesting that the virus was already circulating in the population. While other variants have been detected since then, such as the Beta (B.1.351) and Gamma (P.1) variants [38], Alpha accounted for majority of the identified known VOC cases in Ontario over the second wave owing to its higher transmissibility. As of March 28, 2021, over 92% of the cases were caused by the Alpha variant [39]. This dominance trend of Alpha in Ontario carried on towards the third wave, with an alarming 4,736 new cases recorded at its peak in April 15, 2021 [40].

While case counts in the province have lowered after this third wave, reaching as low as 306 new cases in October 2021 [41], the domination of the more transmissible Delta (B.1.617.2) variant, as well as the gradual re-opening of the province and lifting of public health measures, have caused a new wave of infections to be recorded. On November 15, 2021, it was reported that the Delta variant comprised an estimated 99.3% of the recorded cases in Ontario [42].

The first recorded cases of the Omicron (B.1.1.529) variant in the province, which is the most recent VOC, were identified on November 28, 2021, and attributed to two people from Ottawa, Ontario who have travelled to Nigeria [43]. Because of its even higher transmissibility,

Table 2.1: The three-stage vaccination strategy implemented in Ontario. [47]

Phase 1 (High-risk populations)	Phase 2 (Mass delivery)	Phase 3 (Steady state)
December 2020 – March 2021	April 2021 – June 2021	July 2021 onwards
Seniors in congregate living	Adults aged 55 and older, in decreasing increments	
Health care workers	People in shelters/group homes (high-risk congregate)	
First Nations, Metis, Inuit adults	Individuals with certain health conditions	All remaining eligible Ontarians
Adults aged 80 and older	Certain essential caregivers	
	People living in hot spot communities	
	People who cannot work from home	

Omicron has quickly taken over Delta as the dominant variant and spearheaded the fifth wave of the pandemic, infecting an estimate of 3.5 times more individuals in a two-month span compared to Delta [44]. On December 31, 2021, a record 18,445 new cases were recorded, with more cases potentially not recorded due to changes in testing availability [45]. Cases have been declining throughout the year after the Omicron BA.1 variant, and despite cases of new Omicron variants being discovered in the province, reported case counts have not reached the level of the initial Omicron wave. Currently, the Omicron BA.5 variant is expected to dominate COVID-19 cases in Ontario, with immunity generated by previous infections or vaccination being weaker than earlier variants [46].

2.2   Vaccination strategies and timelines

Table 2.1 shows the three-stage vaccination strategy that the Ontario government developed and implemented in order to rise the population immunity against COVID-19 [47]. Ontario started COVID-19 vaccine roll-out in December 2020, focusing on high-risk populations such as LTCH residents, front-line healthcare workers, chronic home care recipients, First Nations, Métis, and Inuit adults, and adults aged 80 years and older [47].

Vaccines against COVID-19 that were approved for distribution in Ontario fall under

Table 2.2: Timeline of vaccine eligibility for different age groups in Ontario (excluding high-risk populations and those living in "hot-spot" regions). [47, 49]

Age Group	Date (Pfizer-BioNTech)	Date (Moderna)	Date (AstraZeneca)
80+	15 March 2021	15 March 2021	22 March 2021
75-79	22 March 2021	22 March 2021	22 March 2021
70-74	27 March 2021	27 March 2021	22 March 2021
60-69	02 April 2021	02 April 2021	22 March 2021
55-59	30 April 2021	30 April 2021	03 April 2021
50-54	06 May 2021	06 May 2021	20 April 2021
40-49	13 May 2021	13 May 2021	20 April 2021
18-44	18 May 2021	13 May 2021	NA
12-17	23 May 2021	NA	NA

two different categories: messenger RNA (mRNA) and non-replicating viral vector vaccines [48]. The Moderna and Pfizer-BioNTech vaccines, approved by Health Canada in December 2020, are both mRNA, and administered in two doses with a 28-day and 21-day time interval between the first and second doses, respectively. While both vaccines employ the same mechanism, there were differences in efficacy estimates against infection, symptomatic disease, and severe disease. The Astra-Zeneca vaccine, approved for distribution later in March 2021, falls under the viral vector category. While it also follows a two-dose schedule for full vaccine effectiveness, the authorised interval between doses is longer, ranging from 4 to 12 weeks [48].

Despite early authorisation by Health Canada, the initial limited supply of mRNA vaccines in Canada prompted the Ontario government to prioritize the most vulnerable population, in order to reduce COVID-19 hospitalisations, ICU admissions, and deaths among high risk individuals [50]. The vaccine roll-out for the rest of the population was then followed in a decreasing order of age groups, and patterned after the scheduled delivery of vaccine supply

to Canada [47]. Table 2.2 shows the timelines of vaccine eligibility for different age groups [47, 49], which did not apply to people who were part of the high-risk populations as mentioned earlier, nor those who resided in areas where the province deemed as "hot-spots" for which timelines were accelerated [51].

Cases of vaccine-induced prothrombotic immune thrombocytopenia (VIPIT), or rare blood clots, among women below the age of 55 who received the Astra-Zeneca COVID-19 vaccine have been reported in Europe in March 2021 [52], at the time when Canada was able to procure supply of the vaccine. With the likelihood of VIPIT occurrence ranging from 1 in 26,500 to 1 in 127,300 first doses administered [53], the National Advisory Committee on Immunization (NACI) recommended the pause of administering the Astra-Zeneca vaccine to individuals younger than 55 years of age as a precautionary measure on March 29, 2021 [54]. On April 20, 2021, Ontario lowered the age eligibility for the Astra-Zeneca vaccine from 55 years to 40 years, following a statement by Health Canada not restricting administration of the vaccine by age or sex [55]. Finally, on May 11, 2021, it was decided that Ontario will no longer provide the first dose of the Astra-Zeneca vaccine to the public, and that those who require the second dose would be allowed to be vaccinated with either of the mRNA vaccines available as of June 1, 2021 [55, 56]. Due to this interruption in Astra-Zeneca vaccine distribution in Canada, we focus on mRNA vaccines in this thesis.

As mentioned previously, the recommended interval between doses of the Pfizer-BioNTech and Moderna vaccines in primary series are 21 and 28 days, respectively. However, due to inadequate supply, and to allow a greater percentage of the population with partial immunity against COVID-19, this interval was extended to up to 4 months [57]. On June 21, 2021, with the province achieving a 75% first-dose coverage of the eligible population and an increased supply of vaccines being shipped, the second dose administration was then changed to follow the recommended intervals based on clinical trials, allowing partially-vaccinated individuals to receive the second dose on schedule [58].

With the rise of more transmissible SARS-CoV-2 variants, and with studies showing potential waning immunity after vaccination [59, 60], the province began to distribute vaccine booster doses (third dose) on November 6, 2021, targeting the same high-risk population identified during the first stage of vaccine distribution in 2021 [61]. Booster eligibility was again expanded on a decreasing age group basis, and on December 20, 2021, all fully-vaccinated adults (18+ years old) became eligible to receive the booster dose, provided that it a minimum of 180 days (6 months) had elapsed since the second dose of primary series [62].

Tables 2.3 and 2.4 show the efficacies of Moderna and Pfizer-BioNTech vaccines against infection, symptomatic disease, and severe disease for each of the SARS-CoV-2 variants considered in this thesis. For both vaccines, the efficacy against symptomatic disease is conditional on the individual becoming infected (i.e. coming from the latent stage), and the efficacy against severe disease is conditional on the infected individual exhibiting symptoms (i.e. coming from the pre-symptomatic stage).

Table 2.3: Moderna vaccine efficacy against select variants. Unless values are assumed, 95% confidence intervals are given in parentheses. [63, 64]

Vaccine Efficacy (Moderna)	Days after the first dose		Days after the second dose	
Original strain	1-14	>14	1-14	>14
Infection	None	84 (66, 93)	84 (assumed)	96 (91, 99)
Symptomatic disease	None	63 (47, 74)	70 (51, 81)	96 (85, 99)
Severe disease	None	66 (43, 80)	70 (41, 85)	97 (78, 100)
Alpha	1-14	>14	1-14	>14
Infection	None	90 (83, 94)	90 (assumed)	98 (97, 99)
Symptomatic disease	None	82 (80, 84)	83 (80, 85)	92 (88, 95)
Severe disease	None	80 (76, 84)	82 (77, 86)	95 (92, 97)
Delta	1-14	>14	1-14	>14
Infection	None	77 (61, 87)	77 (assumed)	87 (84, 89)
Symptomatic disease	None	70 (64, 76)	69 (62, 75)	95 (91, 97)
Severe disease	None	90 (82, 94)	91 (83, 95)	98 (93, 99)

Table 2.4: Pfizer-BioNTech vaccine efficacy against select variants. Unless values are assumed, 95% confidence intervals are given in parentheses. [64–67]

Vaccine Efficacy (Pfizer-BioNTech)	Days after the first dose		Days after the second dose	
Original strain	1-14	>14	1-14	>14
Infection	None	46 (40, 51)	46 (assumed)	86 (82, 89)
Symptomatic disease	None	63 (56, 68)	65 (58, 71)	93 (88, 95)
Severe disease	None	77 (67, 84)	88 (79, 94)	98 (90, 99)
Alpha	1-14	>14	1-14	>14
Infection	None	29 (23, 35)	29 (assumed)	89 (86, 92)
Symptomatic disease	None	67 (65, 68)	70 (69, 72)	89 (87, 90)
Severe disease	None	82 (81, 84)	87 (85, 88)	96 (94, 97)
Delta	1-14	>14	1-14	>14
Infection	None	41 (assumed)	41 (assumed)	85 (79, 90)
Symptomatic disease	None	57 (53, 61)	59 (54, 63)	92 (90, 94)
Severe disease	None	81 (76, 85)	81 (76, 85)	97 (96, 98)

Chapter 3

Methods

3.1 Model description

The transmission of SARS-CoV-2 was modelled by extending an age-structured SEIR (Susceptible, Exposed, Infectious, Recovered) model, including additional compartments of asymptomatic, pre-symptomatic, mild/severe symptomatic, and isolation of infected individuals (Figure 3.1). Vaccination dynamics and the potential for reinfection after recovery are also implemented in the model. The total population was divided into seven age groups of 0-4, 5-11, 12-17, 18-49, 50-64, 65-79, and 80+ years old, with demographics of births and non-COVID-19 deaths omitted assuming a constant population size.

3.1.1 Model assumptions

The following key assumptions were made in constructing the model:

- Asymptomatic and mildly symptomatic individuals do not require hospitalisation.

- Severe cases that are not hospitalised will remain in self-isolation until recovery.

Table 3.1: Description of the basic model state variables. Variables corresponding to individuals identified and isolated directly from latency are denoted with $\widehat{X}$, while those identified and isolated during the infectious period (A, P, I_m, I_s) are denoted with $\check{X}$.

Variable	Description
S_a	susceptible in age group a
S_{ra}	susceptible in age group a (reinfection/waning immunity)
V_{1a}	vaccinated in age group a (1st dose)
V_{2a}	vaccinated in age group a (2nd dose)
E_a	exposed in age group a (without vaccination)
$\mathcal{E}_{V1a}$	exposed in age group a (vaccinated, 1st dose)
$\mathcal{E}_{V2a}$	exposed in age group a (vaccinated, 2nd dose)
A_a	asymptomatic in age group a
P_a	pre-symptomatic in age group a
I_{ma}	mild symptomatic in age group a
I_{sa}	severe symptomatic in age group a
H_a	hospitalised in age group a
D_a	dead in age group a
R_a	recovered in age group a
N_a	population size of age group a
$M_{a,j}$	contact rate for non-isolated individuals in age groups a and j
$\widetilde{M}_{a,j}$	contact rate for isolated individuals in age groups a and j
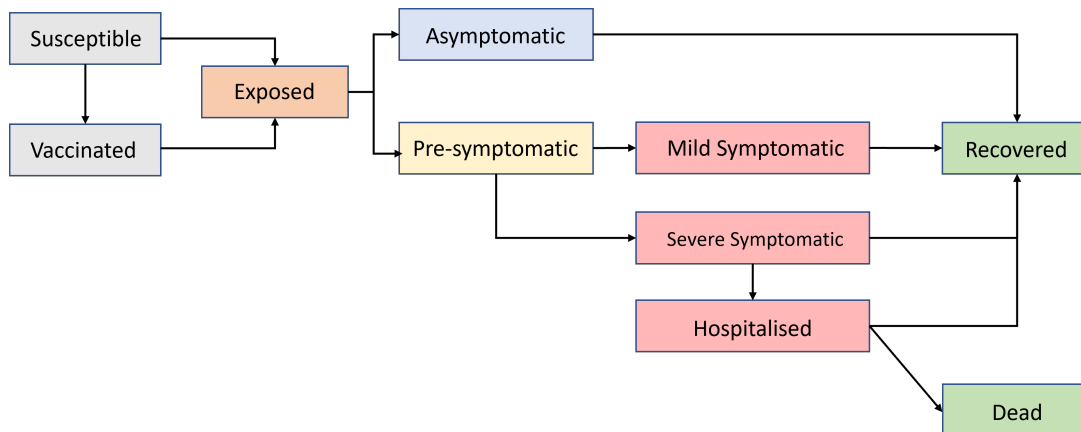
Figure 3.1: A basic schematic diagram of the model dynamics.

- Infected individuals who are identified and isolated (regardless of disease compartment) will remain isolated until recovery, with reduced daily contacts $\widetilde{M}_{a,j}$.

- Hospitalised individuals are assumed to be perfectly isolated and are not included in the force of infection $\mathcal{J}_a$.

- Only hospitalised individuals are at risk of death.

3.1.2   Susceptible and vaccinated individuals

Without any immunity (prior infection or vaccination), individuals are susceptible to contracting COVID-19. Once infected, individuals move to the exposed (latent) class E_a, for age group a. The transmission of disease depends on whether susceptible individuals come in contact with infected individuals before or during the isolation period. The force of infection $\mathcal{J}_a$, or the rate at which susceptible individuals in age group a become infected, is obtained as follows:

$$
\begin{aligned}
\mathcal{J}_a = {} & \beta \sum_{j=1}^{6} M_{a,j} \left(\frac{P_j + \alpha A_j + \kappa I_{mj} + \zeta I_{sj}}{N_j} \right) \\
& + \beta \sum_{j=1}^{6} \widetilde{M}_{a,j} \left(\frac{\widehat{P}_j + \alpha \widehat{A}_j + \kappa \widehat{I}_{mj} + \zeta \widehat{I}_{sj} + \breve{P}_j + \alpha \breve{A}_j + \kappa \breve{I}_{mj} + \zeta \breve{I}_{sj}}{N_j} \right),
\end{aligned}
\tag{3.1}
$$

where P_j, A_j, I_{mj} and I_{sj} are the infected individuals in age group j described in Table 3.1, $\widehat{P}_j$, $\widehat{A}_j$, $\widehat{I}_{mj}$ and $\widehat{I}_{sj}$ are the infected individuals who were identified and isolated during the latent period, and $\breve{P}_j$, $\breve{A}_j$, $\breve{I}_{mj}$ and $\breve{I}_{sj}$ are the infected individuals who were identified and isolated during their respective infectious periods. The contact rates between individuals in age groups a and j are denoted by $M_{a,j}$ for non-isolated individuals, and $\widetilde{M}_{a,j}$ for isolated individuals (see section 3.3.2 for Contact Matrices). The parameters β, α, κ and ζ are related to transmissibility of infections, and are described in Table 3.2.

Vaccination was implemented in the model as a two-dose strategy. The first dose of the vaccine was administered to susceptible individuals (S_a) at a rate of ξ_a, moving to the V_{1a} class. These newly vaccinated individuals then obtain partial immunity against infection and disease 14 days after vaccination. The second dose of the vaccine was administered $1/\nu$ days after the first dose (which depended on the type of vaccine), moving individuals to the V_{2a} class. 7 days after obtaining the second dose, vaccinated individuals will obtain full immunity. Individuals can also be infected after vaccination, and will then move to the exposed class, similar to those unvaccinated who acquire infection. Moreover, waning immunity can occur in fully-vaccinated individuals; these individuals will not go back to S_a, but rather have their own susceptible class S_{ra} (see Section 3.1.8). We denote the average duration of protection by $1/\lambda$ (days). The dynamics of these classes are described by the following equations:

$$
S_a' = -S_a \mathcal{J}_a - \xi_a S_a
\tag{3.2}
$$

$$V'_{1a} = \xi_a S_a - V_{1a} \mathcal{J}_a - \nu V_{1a} \tag{3.3}$$

$$V'_{2a} = \nu V_{1a} - (1 - \epsilon_2) V_{2a} \mathcal{J}_a - \lambda V_{2a} \tag{3.4}$$

3.1.3 Infected, latent stage

Susceptible, partially-vaccinated, and fully-vaccinated individuals who are infected remain in the latent stages of E_a, $\mathcal{E}_{V1a}$ and $\mathcal{E}_{V2a}$, respectively, for an average duration of $1/\sigma$ days. During this period, it is also possible for a fraction q_a of these individuals to be identified and isolated for the duration of the disease, denoted by $\widehat{E}_a$, $\widehat{\mathcal{E}}_{V1a}$, and $\widehat{\mathcal{E}}_{V2a}$.

$$E'_a = (1 - q_a) S_a \mathcal{J}_a - \sigma E_a \tag{3.5}$$

$$\mathcal{E}'_{V1a} = (1 - q_a)(1 - \epsilon_1) V_{1a} \mathcal{J}_a - \sigma \mathcal{E}_{V1a} \tag{3.6}$$

$$\mathcal{E}'_{V2a} = (1 - q_a)(1 - \epsilon_2) V_{2a} \mathcal{J}_a - \sigma \mathcal{E}_{V2a} \tag{3.7}$$

$$\widehat{E}'_a = q_a S_a \mathcal{J}_a - \sigma \widehat{E}_a \tag{3.8}$$

$$\widehat{\mathcal{E}}'_{V1a} = q_a(1 - \epsilon_1) V_{1a} \mathcal{J}_a - \sigma \widehat{\mathcal{E}}_{V1a} \tag{3.9}$$

$$\widehat{\mathcal{E}}'_{V2a} = q_a(1 - \epsilon_2) V_{2a} \mathcal{J}_a - \sigma \widehat{\mathcal{E}}_{V2a} \tag{3.10}$$

3.1.4 Asymptomatic stage

A proportion p_a of infectious individuals who are not identified during the latent stage $(E_a, \mathcal{E}_{V1a}, \mathcal{E}_{V2a})$ and those identified and isolated during the latent stage $(\widehat{E}_a, \widehat{\mathcal{E}}_{V1a}, \widehat{\mathcal{E}}_{V2a})$ exhibit no symptoms over the course of infection, and therefore move to asymptomatic classes A_a and $\widehat{A}_a$, respectively. These individuals remain infectious for an average duration of $1/\eta$ days before recovery. It is also possible to identify a proportion g_a of asymptomatic individuals with a delay of $1/\delta$ days from the start of the asymptomatic stage, and thus isolate them (denoted by $\breve{A}_a$) for the remainder of their infectious period, which is $(\delta - \eta)/\delta\eta$

days on average. Thus,

$$A'_a = p_a \sigma E_a + \rho_{1a} \sigma \mathcal{E}_{V1a} + \rho_{2a} \sigma \mathcal{E}_{V2a} - (1 - g_a)\eta A_a - g_a \delta A_a \tag{3.11}$$

$$\widehat{A}'_a = p_a \sigma \widehat{E}_a + \rho_{1a} \sigma \widehat{\mathcal{E}}_{V1a} + \rho_{2a} \sigma \widehat{\mathcal{E}}_{V2a} - \eta \widehat{A}_a \tag{3.12}$$

$$\breve{A}'_a = g_a \delta A_a - \left(\frac{\delta \eta}{\delta - \eta} \right) \breve{A}_a \tag{3.13}$$

3.1.5 Pre-symptomatic stage

A proportion $(1 - p_a)$ of infectious individuals who are not identified during the latent stage $(E_a, \mathcal{E}_{V1a}, \mathcal{E}_{V2a})$ and those identified and isolated during the latent stage $(\widehat{E}_a, \widehat{\mathcal{E}}_{V1a}, \widehat{\mathcal{E}}_{V2a})$ enter the pre-symptomatic stage P_a and $\widehat{P}_a$, where symptoms do not manifest until an average duration of $1/\theta$ days. Similar to the asymptomatic case, it is also possible to identify a proportion g_a of pre-symptomatic individuals $1/\delta$ days from the start of the pre-symptomatic stage, and thus isolate them (denoted by $\breve{P}_a$) for the remainder of their infectious period, which is $(\delta - \theta)/\delta\theta$ days on average. Thus, we get

$$P'_a = (1 - p_a)\sigma E_a + (1 - \rho_{1a})\sigma \mathcal{E}_{V1a} + (1 - \rho_{2a})\sigma \mathcal{E}_{V2a} - g_a \delta P_a - (1 - g_a)\theta P_a \tag{3.14}$$

$$\widehat{P}'_a = (1 - p_a)\sigma \widehat{E}_a + (1 - \rho_{1a})\sigma \widehat{\mathcal{E}}_{V1a} + (1 - \rho_2 a)\sigma \widehat{\mathcal{E}}_{V2a} - \theta \widehat{P}_a \tag{3.15}$$

$$\breve{P}'_a = g_a \delta P_a - \left(\frac{\delta \theta}{\delta - \theta} \right) \breve{P}_a \tag{3.16}$$

3.1.6 Infectious stage with mild illness

After the pre-symptomatic stage, a proportion m_a of individuals will enter the infectious class with mild illness (I_{ma}), and remain infectious for an average period of $1/\gamma$ days before recovering. Those who belong in the isolated pre-symptomatic stages $(\widehat{P}_a, \breve{P}_a)$ remain isolated as they enter this stage, denoted by $\widehat{I}_{ma}$. We assume that a proportion of individuals f_a who have not been identified or isolated during the earlier stages of infection $(\breve{I}_{ma})$ will self-isolate

within $1/\tau$ days of symptom onset, and will remain isolated for an average of $(\tau - \gamma)/\tau\gamma$ days until recovery. The dynamics are therefore governed by

$$I'_{ma} = (1 - g_a)m_a\theta P_a - f_a\tau I_{ma} - (1 - f_a)\gamma I_{ma} \tag{3.17}$$

$$\widehat{I}'_{ma} = m_a\theta\widehat{P}_a + m_a\left(\frac{\delta\theta}{\delta - \theta}\right)\widecheck{P}_a - \gamma\widehat{I}_{ma} \tag{3.18}$$

$$\widecheck{I}'_{ma} = f_a\tau I_{ma} - \left(\frac{\tau\gamma}{\tau - \gamma}\right)\widecheck{I}_{ma} \tag{3.19}$$

3.1.7   Infectious stage with severe illness

After the pre-symptomatic stage, a proportion $(1 - m_a)$ of individuals will enter the infectious class with severe illness (I_{sa}). We assume that a proportion h_a of these individuals will be hospitalised (H_a) with an average time of $1/\omega$ days after symptom onset. The remainder of these cases are assumed to self-isolate within $1/\tau$ days of symptom onset (denoted by $\widecheck{I}_{sa}$) for an average time of $(\tau - \gamma)/\tau\gamma$ days until recovery.

Those who belong in the isolated pre-symptomatic stages ($\widehat{P}_a$, $\widecheck{P}_a$) also remain isolated as they enter this stage, denoted by $\widehat{I}_{sa}$. Similar to those coming from non-isolated pre-symptomatic stages, a proportion h_a will be hospitalised $1/\omega$ days after symptom onset, while the remaining proportion will continue to self-isolate for an average period of $1/\gamma$ days until recovery. This gives:

$$I'_{sa} = (1 - g_a)(1 - m_a)\theta P_a - (1 - h_a)\tau I_{sa} - h_a\omega I_{sa} \tag{3.20}$$

$$\widehat{I}'_{sa} = (1 - m_a)\theta\widehat{P}_a + (1 - m_a)\left(\frac{\delta\theta}{\delta - \theta}\right)\widecheck{P}_a - (1 - h_a)\gamma\widehat{I}_{sa} - h_a\omega\widehat{I}_{sa} \tag{3.21}$$

$$\widecheck{I}'_{sa} = (1 - h_a)\tau I_{sa} - \left(\frac{\tau\gamma}{\tau - \gamma}\right)\widecheck{I}_{sa} \tag{3.22}$$
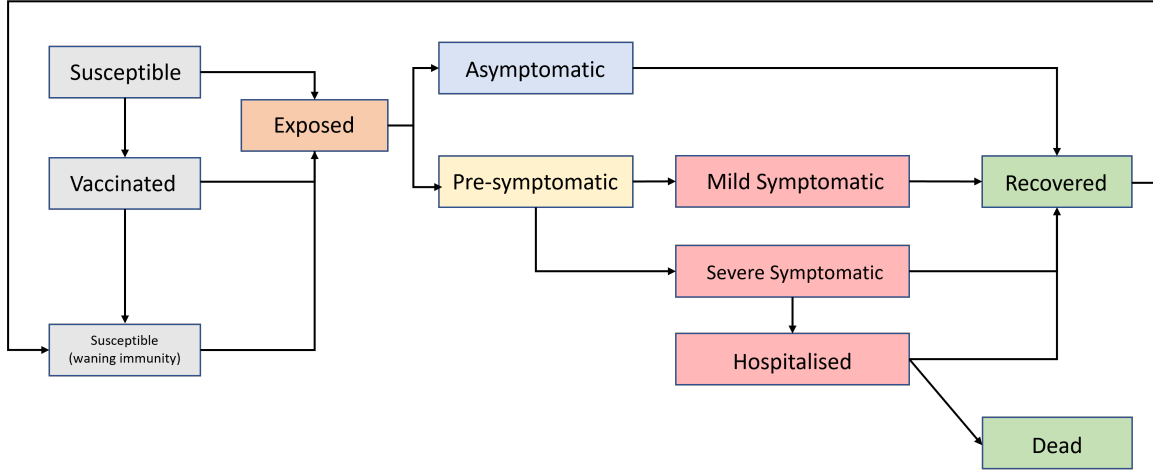
Figure 3.2: A basic schematic diagram of the model dynamics with waning immunity and reinfection.

3.1.8   Waning immunity and reinfection

We also consider a scenario in which immunity wanes over time with an average of $1/\lambda$ days for the duration of protection after beging fully vaccinated or recovered from infection (Figure 3.2). These individuals are considered to have the same immunity level as those in the V_{1a} class, and whose disease dynamics for reinfection are described as follows:

$$S'_{ra} = \lambda V_{2a} + \lambda R_a - (1 - \epsilon_1)S_{ra}\mathcal{J}_a \tag{3.23}$$

In this scenario, equations (3.6) and (3.9) for exposed individuals will be modified to include reinfections:

$$\mathcal{E}'_{V1a} = (1 - q_a)(1 - \epsilon_1)(V_{1a} + S_{ra})\mathcal{J}_a - \sigma\mathcal{E}_{1a} \tag{3.24}$$

$$\widehat{\mathcal{E}}'_{V1a} = q_a(1 - \epsilon_1)(V_{1a} + S_{ra})\mathcal{J}_a - \sigma\widehat{\mathcal{E}}_{1a} \tag{3.25}$$

3.1.9 Hospitalisation, death, and recovery

For both primary infections and reinfections, a proportion h_a of individuals with severe illness require hospitalisation (H_a), where a proportion d_a eventually die (D_a) after an average of $1/\phi$ days. The remaining cases $(1 - d_a)$ recover after an average of $1/\psi$ days. Other infected individuals eventually recover in the class R_a, with the dynamics as described below:

$$H_a' = h_a \omega I_{sa} + h_a \omega \widehat{I}_{sa} - (1 - d_a)\psi H_a - d_a \phi H_a \tag{3.26}$$

$$D_a' = d_a \phi H_a \tag{3.27}$$

$$R_a' = (1 - g_a)\eta A_a + (1 - f_a)\gamma I_{ma} + \left(\frac{\tau\gamma}{\tau - \gamma}\right)\left(\breve{I}_{ma} + \breve{I}_{sa}\right) + \eta \widehat{A}_a$$
$$+ \left(\frac{\delta\eta}{\delta - \eta}\right)\breve{A}_a + \gamma \widehat{I}_{ma} + (1 - h_a)\gamma \widehat{I}_{sa} + (1 - d_a)\psi H_a - \lambda R_a \tag{3.28}$$

In summary, equations (3.2) to (3.28) comprise the entire model dynamics for each age-group.

3.2 Model extension: multiple variants

In the case where there are two variants of the same disease present in the population, with different transmissibilities β_1 and β_2, the force of infection $\mathcal{J}_a$ (equation 3.1) will then be modified to account for the interaction with infectious individuals with different variants (with subscripts 1 and 2 corresponding to the variants):

$$\begin{aligned}
\mathcal{J}_{1a} = \beta_1 \sum_{j=1}^{6} M_{a,j} \left(\frac{P_{1j} + \alpha A_{1j} + \kappa I_{m1j} + \zeta I_{s1j}}{N_j}\right) \\
+ \beta_1 \sum_{j=1}^{6} \widetilde{M}_{a,j} \left(\frac{\widehat{P}_{1j} + \alpha \widehat{A}_{1j} + \kappa \widehat{I}_{m1j} + \zeta \widehat{I}_{s1j} + \breve{P}_{1j} + \alpha \breve{A}_{1j} + \kappa \breve{I}_{m1j} + \zeta \breve{I}_{s1j}}{N_j}\right)
\end{aligned} \tag{3.29}$$

$$\mathcal{J}_{2a} = \beta_2 \sum_{j=1}^{6} M_{a,j} \left(\frac{P_{2j} + \alpha A_{2j} + \kappa I_{m2j} + \zeta I_{s2j}}{N_j} \right)$$
$$+ \beta_2 \sum_{j=1}^{6} \widetilde{M}_{a,j} \left(\frac{\widehat{P}_{2j} + \alpha \widehat{A}_{2j} + \kappa \widehat{I}_{m2j} + \zeta \widehat{I}_{s2j} + \breve{P}_{2j} + \alpha \breve{A}_{2j} + \kappa \breve{I}_{m2j} + \zeta \breve{I}_{s2j}}{N_j} \right) \tag{3.30}$$

Equations 3.2 to 3.4 are then slightly modified, with $\mathcal{J}_a = \mathcal{J}_{1a} + \mathcal{J}_{2a}$. For each variant, the model dynamics for the exposed and infectious (asymptomatic, pre-symptomatic, symptomatic mild/severe) classes are similar to those in equations 3.5 to 3.22.

3.3   Model parameters

3.3.1   Disease parameters

Parameter values corresponding to COVID-19 dynamics were taken from previous published studies. Parameters that do not vary with age groups are outlined in Table 3.2.

Table 3.2: Description of the model parameters and their values.

Parameter	Description	Value	Reference
β	Transmission rate during pre-symptomatic period	0.06	calibrated to $\mathcal{R}_0 = 2.5$
α	Relative transmissibility of asymptomatic infection	0.26	[26]
κ	Relative transmissibility of mild symptomatic infection	0.44	[27, 28]
ζ	Relative transmissibility of severe symptomatic infection	0.89	[27, 29]
$1/\sigma$	Mean latent period	2.2 days	[68]
$1/\eta$	Mean infectious period of asymptomatic infection	5 days	[69, 70]
$1/\delta$	Time to identification of silent infections	0.8-2.8 days	Assumed
$1/\theta$	Mean duration of pre-symptomatic stage	2.3 days	[28]
$1/\tau$	Mean time to self-isolation post-symptom onset	1 day	Assumed
$1/\gamma$	Mean infectious period post-symptom onset	3.2 days	[70]
$1/\omega$	Mean time to hospitalisation	3.5 days	[71]
$1/\psi$	Mean hospitalisation period without death	12.4 days	[71]
$1/\phi$	Mean hospitalisation period with death	8 days	[71]
$1/\lambda$	Mean duration of immune protection against reinfection	90-180 days	Varied

Table 3.3: Description of the disease-related age-specific model parameters.

Parameter	Description
q_a	Proportion of infected individuals identified during latent period
p_a	Proportion of infected individuals that are asymptomatic
g_a	Proportion of individuals identified during asymptomatic/pre-symptomatic stages
f_a	Proportion of symptomatic cases who self-isolate
m_a	Proportion of infected individuals that are mild symptomatic
h_a	Proportion of severe infected individuals who are hospitalised
d_a	Proportion of severe infected individuals who die

Table 3.4: Values of the disease-related age-specific model parameters.

Parameter	0-4	5-11	12-17	18-49	50-64	65-79	80+	Reference
q_a				0–1				Varied
p_a	0.467	0.467	0.467	0.321	0.321	0.197	0.197	[72]
g_a				0–1				Varied
f_a				1.0				Assumed
m_a	0.95	0.95	0.9	0.85	0.6	0.2	0.2	[29]
h_a	0.001	0.001	0.01	0.1	0.2	0.4	0.8	[29]
d_a	0.0013	0.0013	0.13	0.13	0.26	0.52	0.78	Assumed

3.3.2 Contact matrices

In order to implement heterogeneity in contacts among age groups, two age-specific daily contact matrices were used: a regular contact matrix M for non-isolated individuals, and a reduced contact matrix $\widetilde{M}$ for isolated individuals. The $(a, j)th$ entry of these matrices correspond to the average number of contacts that an individual in age group a has with

individuals in age group j. These matrices were based on a previous study [72] which involves heterogeneous contact patterns within the community [73] and with control measures in place such as isolation [74].

$$
M = \begin{array}{c}
\begin{array}{ccccccc} 0-4 & 5-11 & 12-17 & 18-49 & 50-64 & 65-79 & 80+ \quad \textbf{Age} \end{array} \\
\left[\begin{array}{ccccccc}
1.7364 & 0.5926 & 0.1851 & 1.9849 & 0.6267 & 0.1761 & 0.0186 \\
0.6939 & 2.8578 & 0.9209 & 2.6959 & 0.6223 & 0.2326 & 0.0258 \\
0.1120 & 0.4993 & 3.7604 & 2.9697 & 0.7460 & 0.2812 & 0.0514 \\
0.5103 & 0.5888 & 1.3325 & 6.5946 & 1.8369 & 0.7097 & 0.1560 \\
0.3360 & 0.2824 & 0.7439 & 3.9394 & 2.4118 & 1.1464 & 0.3701 \\
0.0739 & 0.0802 & 0.1792 & 1.0953 & 0.8241 & 1.3806 & 0.2967 \\
0.0197 & 0.0230 & 0.1047 & 0.6479 & 0.7185 & 0.8967 & 0.5795
\end{array}\right]
\begin{array}{l} 0-4 \\ 5-11 \\ 12-17 \\ 18-49, \\ 50-64 \\ 65-79 \\ 80+ \end{array}
\end{array}
$$

$$
\widetilde{M} = \begin{array}{c}
\begin{array}{ccccccc} 0-4 & 5-11 & 12-17 & 18-49 & 50-64 & 65-79 & 80+ \quad \textbf{Age} \end{array} \\
\left[\begin{array}{ccccccc}
0.4500 & 0.2001 & 0.1100 & 1.0101 & 0.2200 & 0.1400 & 0.0098 \\
0.4101 & 0.5800 & 0.3800 & 1.0100 & 0.1800 & 0.2000 & 0.0299 \\
0.0653 & 0.2841 & 0.9606 & 0.7874 & 0.2415 & 0.1408 & 0.0304 \\
0.3291 & 0.3359 & 0.4478 & 1.1559 & 0.3071 & 0.1737 & 0.0705 \\
0.2454 & 0.1452 & 0.4338 & 0.8613 & 0.7440 & 0.3921 & 0.1782 \\
0.0493 & 0.0549 & 0.1060 & 0.3334 & 0.1989 & 0.6781 & 0.1294 \\
0.0100 & 0.0199 & 0.0599 & 0.1900 & 0.3100 & 0.3700 & 0.3101
\end{array}\right]
\begin{array}{l} 0-4 \\ 5-11 \\ 12-17 \\ 18-49 \\ 50-64 \\ 65-79 \\ 80+ \end{array}
\end{array}
$$

3.3.3 Vaccine parameters

The vaccine-related parameter values used in the model are based on the timelines and types of vaccines distributed in Ontario, as discussed in Chapter 2.

Table 3.5: Description of the vaccine-related model parameters.

Parameter	Description
ξ_a	Vaccination rate, calculated to achieve a specific coverage after one year
$1/\nu$	Time between doses
ϵ_1	Vaccine efficacy in preventing infection (14 days after the first dose)
ϵ_2	Vaccine efficacy in preventing infection (7 days after the second dose)
ρ_{1a}	Probability of becoming asymptomatic after infection (after the first dose)
ρ_{2a}	Probability of becoming asymptomatic after infection (after the second dose)

Values used for ρ_{1a} and ρ_{2a} were calculated as follows, with values for p_a and VE_{symp} taken from Table 3.4 and Tables 2.3-2.4 respectively:

$$\text{Probability of being symptomatic} = 1 - p_a$$

$$\text{Vaccine efficacy against symptomatic disease (after infection)} = \text{VE}_{symp}$$

$$\text{Probability of asymptomatic disease for age } a = 1 - (1 - p_a)(1 - \text{VE}_{symp}) = \rho_a$$

3.4 Non-standard method for numerical solutions

A first-order nonstandard method of discretisation was used to solve the model numerically, as outlined in [75]. This method was chosen in order to mitigate problems which can occur with more standard approaches. In particular, since each equation in the model deals with populations, the solutions must be positive for each iteration, which is guaranteed by using the non-standard method.

Table 3.6: Values of the vaccine-related model parameters.

Parameter	Value (Moderna)	Value (Pfizer-BioNTech)
$1/\nu$	28 days	21 days
ϵ_1 (Original strain)	0.84	0.46
ϵ_1 (Alpha)	0.90	0.29
ϵ_1 (Delta)	0.77	0.41
ϵ_2 (Original strain)	0.96	0.86
ϵ_2 (Alpha)	0.98	0.89
ϵ_2 (Delta)	0.87	0.85
ρ_{1a}	$p_a \leq \rho_{1a} \leq 100\%$	$p_a \leq \rho_{1a} \leq 100\%$
ρ_{2a}	$p_a \leq \rho_{2a} \leq 100\%$	$p_a \leq \rho_{2a} \leq 100\%$

The following rules are applied in discretisation [75]:

(a) all negative terms of the variable x being approximated should be written in the advanced time-step $(t_{i+1} = t_i + h)$ factored out, where h is the step size;

(b) for negative terms of x with order $n > 1$ (i.e. $x^n = x \cdot x^{n-1}$): order 1 x is approximated in an advanced time-step t_{i+1} (i.e. $x(t_{i+1})$), and the remaining x^{n-1} will be approximated at the current time-step t_i (i.e. $[x(t_i)]^{n-1}$);

(c) every other variable not x in the equation is approximated in the current time-step t_i.

Applying the rules to each equation in the model, and setting $x(t_{i+1}) = x(t_i + h)$ for a fixed time-step h, the discretised form of equations (3.1) to (3.28) for each age group is given by:

$$\mathcal{J}_a(t_i) = \beta \sum_{j=1}^{6} M_{a,j} \left(\frac{P_j(t_i) + \alpha A_j(t_i) + \kappa I_{mj}(t_i) + \zeta I_{sj}(t_i)}{N_j} \right)$$

$$+ \beta \sum_{j=1}^{6} \widetilde{M}_{a,j} \left(\frac{\widehat{P}_j(t_i) + \alpha \widehat{A}_j(t_i) + \kappa \widehat{I}_{mj}(t_i) + \zeta \widehat{I}_{sj}(t_i) + \breve{P}_j(t_i) + \alpha \breve{A}_j(t_i) + \kappa \breve{I}_{mj}(t_i) + \zeta \breve{I}_{sj}(t_i)}{N_j} \right)$$

$$S_a(t_{i+1}) = \frac{S_a(t_i)}{1 + h\mathcal{J}_a(t_i) + h\xi_a}$$

$$S_{ra}(t_{i+1}) = \frac{S_{ra}(t_i) + h\lambda V_{2a}(t_i) + h\lambda R_a(t_i)}{1 + h(1 - \epsilon_{1e})\mathcal{J}_a(t_i)}$$

$$V_{1a}(t_{i+1}) = \frac{V_{1a}(t_i) + h\xi_a S_a(t_i)}{1 + h\mathcal{J}_a(t_i) + h\nu}$$

$$V_{2a}(t_{i+1}) = \frac{V_{2a}(t_i) + h\nu V_{1a}(t_i)}{1 + h(1 - \epsilon_2)\mathcal{J}_a(t_i) + h\lambda}$$

$$E_a(t_{i+1}) = \frac{E_a(t_i) + h(1 - q_a)S_a(t_i)\mathcal{J}_a(t_i)}{1 + h\sigma}$$

$$\mathcal{E}_{V1a}(t_{i+1}) = \frac{\mathcal{E}_{V1a}(t_i) + h(1 - q_a)(1 - \epsilon_1)(V_{1a}(t_i) + S_{ra}(t_i))\mathcal{J}_a(t_i)}{1 + h\sigma}$$

$$\mathcal{E}_{V2a}(t_{i+1}) = \frac{\mathcal{E}_{V2a}(t_i) + h(1 - q_a)(1 - \epsilon_2)V_{2a}(t_i)\mathcal{J}_a(t_i)}{1 + h\sigma}$$

$$\widehat{E}(t_{i+1}) = \frac{\widehat{E}_a(t_i) + hq_a S_a(t_i)\mathcal{J}_a(t_i)}{1 + h\sigma}$$

$$\widehat{\mathcal{E}}_{V1a}(t_{i+1}) = \frac{\widehat{\mathcal{E}}_{V1a}(t_i) + hq_a(1 - \epsilon_1)(V_{1a}(t_i) + S_{ra}(t_i))(t_i)\mathcal{J}_a(t_i)}{1 + h\sigma}$$

$$\widehat{\mathcal{E}}_{V2a}(t_{i+1}) = \frac{\widehat{\mathcal{E}}_{V2a}(t_i) + hq_a(1 - \epsilon_2)V_{2a}(t_i)\mathcal{J}_a(t_i)}{1 + h\sigma}$$

$$A_a(t_{i+1}) = \frac{A_a(t_i) + hp_a\sigma E_a(t_i) + h\rho_{1a}\sigma \mathcal{E}_{V1a}(t_i) + h\rho_{2a}\sigma \mathcal{E}_{V2a}(t_i)}{1 + h(1 - g_a)\eta + hg_a\delta}$$

$$\widehat{A}_a(t_{i+1}) = \frac{\widehat{A}_a(t_i) + hp_a\sigma \widehat{E}_a(t_i) + h\rho_{1a}\sigma \widehat{\mathcal{E}}_{V1a}(t_i) + h\rho_{2a}\sigma \widehat{\mathcal{E}}_{V2a}(t_i)}{1 + h\eta}$$

$$\breve{A}_a(t_{i+1}) = \frac{\breve{A}_a(t_i) + hg_a\delta A_a}{1 + \left(\frac{\delta\eta}{\delta - \eta}\right)}$$

$$P_{1a}(t_{i+1}) = \frac{P_{1a}(t_i) + h(1 - p_a)\sigma E_a(t_i) + h(1 - \rho_{1a})\sigma \mathcal{E}_{V1a}(t_i) + h(1 - \rho_{2a})\sigma \mathcal{E}_{V2a}(t_i)}{1 + hg_a\delta + h(1 - g_a)\theta}$$

$$\widehat{P}_a(t_{i+1}) = \frac{\widehat{P}_{1a}(t_i) + h(1 - p_a)\sigma \widehat{E}_a(t_i) + h(1 - \rho_{1a})\sigma \widehat{\mathcal{E}}_{V1a}(t_i) + h(1 - \rho_{2a})\sigma \widehat{\mathcal{E}}_{V2a}(t_i)}{1 + h\theta}$$

$$\breve{P}_a(t_{i+1}) = \frac{\breve{P}_a(t_i) + hg_a\delta P_a(t_i)}{1 + h\left(\frac{\delta\theta}{\delta - \theta}\right)}$$

$$I_{ma}(t_{i+1}) = \frac{I_{ma}(t_i) + h(1 - g_a)m_a\theta P_a(t_i)}{1 + hf_a\tau + h(1 - f_a)\gamma}$$

$$\widehat{I}_{ma}(t_{i+1}) = \frac{\widehat{I}_{ma}(t_i) + hm_a\theta\widehat{P}_a(t_i) + hm_a\left(\frac{\delta\theta}{\delta-\theta}\right)\widecheck{P}_a(t_i)}{1 + h\gamma}$$

$$\widecheck{I}_{ma}(t_{i+1}) = \frac{\widecheck{I}_{ma}(t_i) + hf_a\tau I_{ma}(t_i)}{1 + h\left(\frac{\tau\gamma}{\tau-\gamma}\right)}$$

$$I_{sa}(t_{i+1}) = \frac{I_{sa}(t_i) + h(1-g_a)(1-m_a)\theta P_a(t_i)}{1 + h(1-h_a)\tau + hh_a\omega}$$

$$\widehat{I}_{sa}(t_{i+1}) = \frac{\widehat{I}_{sa}(t_i) + h(1-m_a)\theta\widehat{P}_a(t_i) + h(1-m_a)\left(\frac{\delta\theta}{\delta-\theta}\right)\widecheck{P}_a(t_i)}{1 + h(1-h_a)\gamma + hh_a\omega}$$

$$\widecheck{I}_{sa}(t_{i+1}) = \frac{\widecheck{I}_{sa}(t_i) + h(1-h_a)\tau I_{sa}(t_i)}{1 + h\left(\frac{\tau\gamma}{\tau-\gamma}\right)}$$

$$H_a(t_{i+1}) = \frac{H_a(t_i) + hh_a\omega(I_{ma}(t_i) + I_{sa}(t_i))}{1 + h(1-d_a)\psi + hd_a\phi}$$

$$D_a(t_{i+1}) = D_a(t_i) + hd_a\phi H_a(t_i)$$

$$R_a(t_{i+1}) = \frac{1}{1+h\lambda}\left[R_a(t_i) + h(1-g_a\eta A_a(t_i) + h(1-f_a)\gamma I_{ma}(t_i) + h\left(\frac{\tau\gamma}{\tau-\gamma}\right)(\widecheck{I}_{ma}(t_i) + \widecheck{I}_{sa}(t_i))\right.$$

$$\left. + h\eta\widehat{A}_a(t_i) + h\left(\frac{\delta\eta}{\delta-\eta}\right)\widecheck{A}_a(t_i) + h\gamma\widehat{I}_{ma}(t_i) + h(1-h_a)\gamma\widehat{I}_{sa}(t_i) + h(1-d_a)\psi H_a(t_i)\right]$$

These equations were implemented in MATLAB© in order to simulate the model and obtain the results.

Chapter 4

Scenarios and Results

4.1   Scenarios

The model was simulated for a number of scenarios to reflect the timelines of COVID-19 outbreaks in Ontario, Canada as of November 1, 2021. Note that while there are other variants of concern that have been identified during this time period since emergence of SARS-CoV-2, this thesis only focused on the variants that dominated pandemic "waves". The summary of these scenarios are provided in Table 4.2.

1. Scenario 1 (S1): Original Wuhan-I strain. Moderna and Pfizer-BioNTech vaccines are administered to the eligible population (ages 12+). Second dose of the vaccine is given either on schedule (4 weeks for Moderna, 3 weeks for Pfizer-BioNTech after the first dose) or with a delay of 8 or 12 weeks.

2. Scenario 2 (S2): the Alpha variant with 50% increased transmissibility relative to original. Same vaccines and second dose schedule as S1.

3. Scenario 3 (S3): the Delta variant, with 30% increased transmissibility relative to the Alpha variant and (a) 20%, (b) 50%, or (c) 80% reduction in vaccine effectiveness.

Vaccines were administered in the same schedules as S1.

4. Scenario 4 (S4): Comprises the Alpha (S2) and Delta (S3) scenarios, with a gap of 120 days between the introduction of each variant into the population. Vaccines were administered in the same schedules as S1.

4.2 Initial conditions for simulations

All simulations were conducted in a synthetic population of 10,000 individuals, which are divided by age groups based on Ontario demographics. At the start of each simulation, one pre-symptomatic infection per age group was introduced, for a total of seven infections in the population. We also run the scenario with different initial conditions (See Appendix A). The pre-existing immunity level (prior to the start of vaccination), which is comprised of previously-infected and recovered individuals, was also fixed before starting the simulations. This level was set to 10% in each scenario unless specified otherwise. Vaccination was then introduced per age group, with the timelines for the first dose shown in Table 4.2. All simulations were run for one year (365 days) for scenarios without re-infection, and two years (730 days) for scenarios with re-infection, with a time step of $h = 0.2$ days (i.e., 4.8 hours).

Table 4.1: Description of simulated scenarios. The last column shows the percentage reduction of vaccine effectiveness.

Scenario	Variant type	Increase in transmissibility	Vaccine type	Time between doses	Reduction in VE
S1	Original	–	Moderna	On schedule	–
			Pfizer-BioNTech	Delayed (8 weeks)	
				Delayed (12 weeks)	
S2	Alpha	50% relative to original	same as S1	same as S1	–
S3.0	Delta	30% relative to Alpha	same as S1	same as S1	0% (no vaccination)
S3.1					20%
S3.2					50%
S3.3					80%
S4.0	Alpha + Delta	same as S2, S3.0-S3.3	same as S1	same as S1	same as S3.0
S4.1					same as S3.1
S4.2					same as S3.2
S4.3					same as S3.3

Table 4.2: Timeline of introduction of vaccine to each age group in the model.

Age Group	Day from start of simulation
80+	30
65-79	37
50-64	48
18-49	89
12-17	99

4.3 Results

4.3.1 Effect of heterogeneity (no control measures)

In the case wherein there are no control measures applied to the population (no vaccination or testing), the herd immunity generated at the end of the epidemic would be determined by the level of pre-existing immunity and the overall attack rate, which is the percentage of the susceptible population that have been infected during the course of the epidemic:

$$\text{Herd immunity} = \text{Pre-existing immunity} + \text{Overall attack rate.}$$

Note that this relation is valid only in the absence of re-infection (i.e., with long-term protection induced by primary infection). Figure 4.1 shows the effect of varying pre-existing immunity to the overall attack rate for each of the three variants. It could be seen that without any level of immunity at the introduction of the disease (0% pre-existing immunity), the overall attack rate was at 47% for the original strain, 57% for the Alpha variant, and 60% for the Delta variant. Meanwhile, using the classical herd immunity equation for homogeneous populations [16], the classical herd immunity values obtained were 60% for the original strain
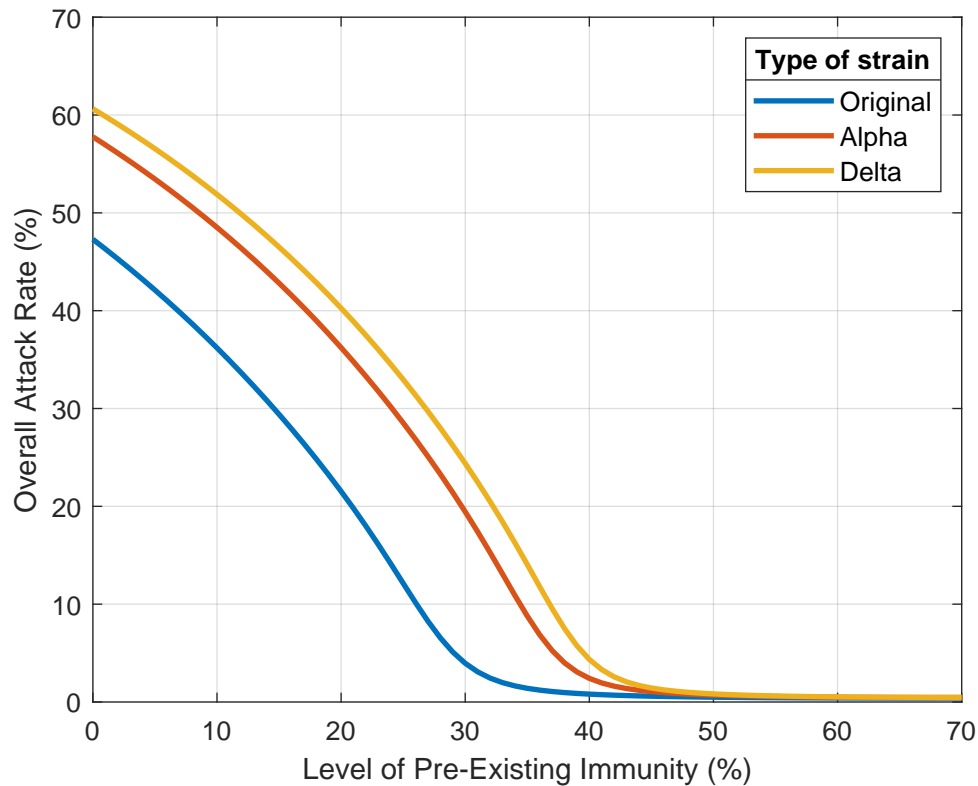
Figure 4.1: Effect of pre-existing immunity on the overall attack rate in the absence of control measures.

($\mathcal{R}_0 = 2.5$), 73.3% for the Alpha variant ($\mathcal{R}_0 = 3.75$), and 79.5% for the Delta variant ($\mathcal{R}_0 = 4.875$).

For the scenario with pre-existing immunity, a similar trend can be observed. For example, for the original variant with 20% pre-existing immunity, the overall attack rate was 20% of the susceptible population. Therefore, the overall herd immunity at the end of a single outbreak was 40%, which was still lower than the classical herd immunity value derived from homogenously mixing population models. In general, higher pre-existing immunity resulted in a lower overall attack rate. Thus, the obtained herd immunity values in this model for all variants were at most at the level of herd immunity calculated for the original strain (lowest transmissibility) with population homogeneity.
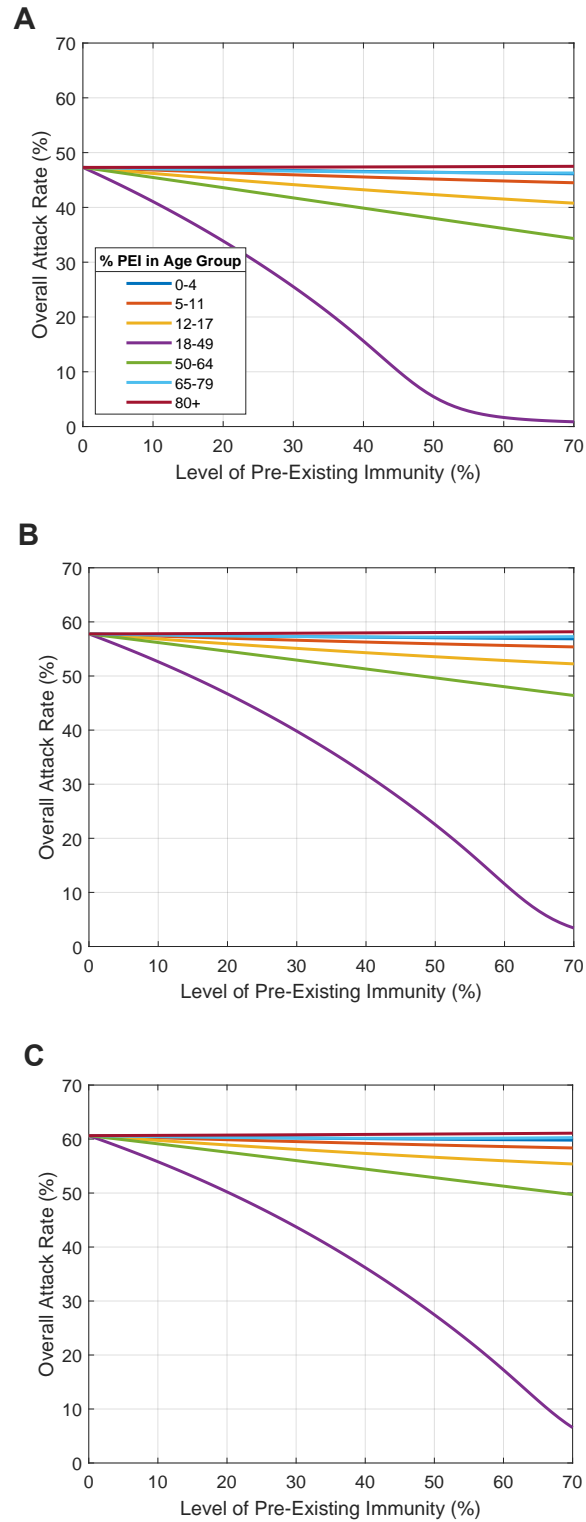
Figure 4.2: Effect of varying pre-existing immunity of specific age groups on overall attack rate of the original (A), Alpha (B), and Delta (C) variants of COVID-19.

To investigate the effect of age-specific pre-existing immunity on the overall attack rate (Figure 4.2), the level of pre-existing immunity for one age group was varied, while leaving the remaining age groups with no pre-existing immunity. We observed that for all variants investigated, the greatest effect was associated with providing pre-existing immunity to the 18-49 age group. This is owing to the size of this age group in the population as compared to other age groups, and their daily number of contacts per individual with other age groups. However, the significance of this effect on the overall attack rate was reduced as the transmissibility of the variant increases. For example, Figure 4.2-C shows that with a 70% pre-existing immunity for the 18-49 age group, the overall attack rate remained several times higher with the Delta variant than with the original strain at the same level of pre-existing immunity (Figure 4.2-A).

4.3.2 Effect of testing and isolation

When the only control measure applied is identification and self-isolation of infections, the resulting overall attack rate was affected by both the level of identification and the time to identification from infection. For all three scenarios simulated, the sharpest declines in attack rate occured when individuals were identified within 2-3 days after infection, while still in the exposed (non-infectious), early asymptomatic, or early pre-symptomatic stages. Longer delays in testing significantly reduced the effect of this measure. Moreover, the identification coverage required to reduce the overall attack rate below a certain level would increase significantly with higher transmissibility of the variant. For example, while a delay of 4 days would result in an overall attack rate of 5% with 60% of the original strain infections identified within 4 days of infection (Figure 4.3-A), the overall attack rate with Alpha and Delta variants were reduced yet remained above 5% even with 100% identification level within 4 days of infection (Figure 4.3-B,C).
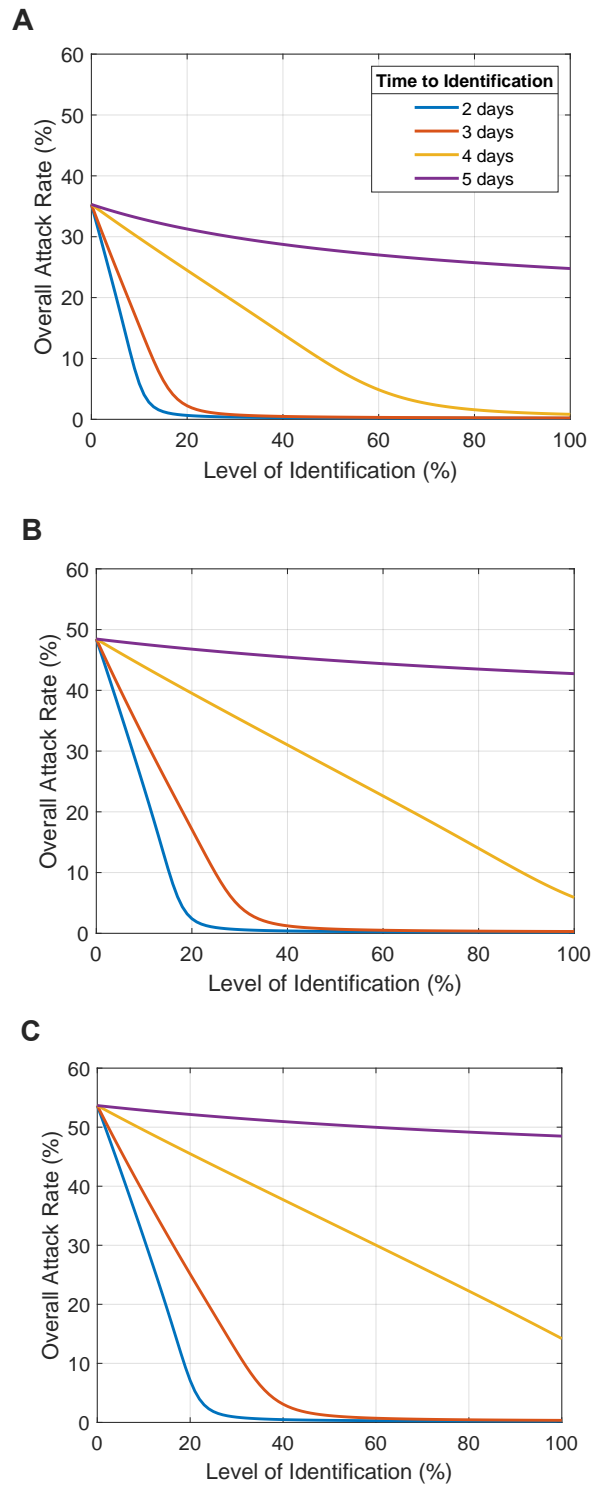
Figure 4.3: Effect of varying identification coverage and time to identification of pre-symptomatic infection on overall attack rate of the original (A), Alpha (B), and Delta (C) variants of COVID-19, with 10% pre-existing immunity in the population.
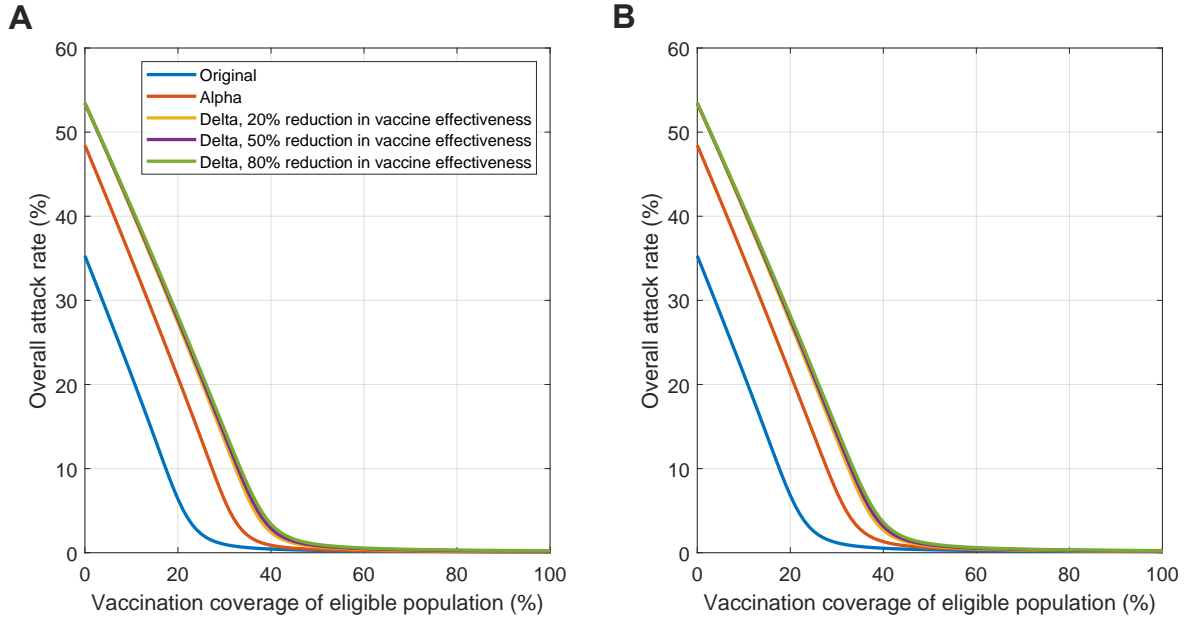
Figure 4.4: Effect of administering (A) Moderna and (B) Pfizer-BioNTech vaccines on the overall attack rate, with 10% pre-existing immunity in the population.

4.3.3 Effect of vaccination

With vaccination as the only control measure, the herd immunity generated at the end of a single outbreak would be determined by the overall vaccination coverage, modifying the expression in Section 4.3.1 to:

$$
\begin{aligned}
\text{Herd immunity} = {} & \text{Pre-existing immunity} \\
& + \Big[(\text{Vaccination coverage of susceptible, previously uninfected individuals}) \\
& \qquad \times (\text{Efficacy of vaccines against infection}) \Big] \\
& + \text{Attack rate.}
\end{aligned}
$$

Note that this relation holds only when the protection conferred by primary infection (or vaccination according to its efficacy) prevents re-infection.
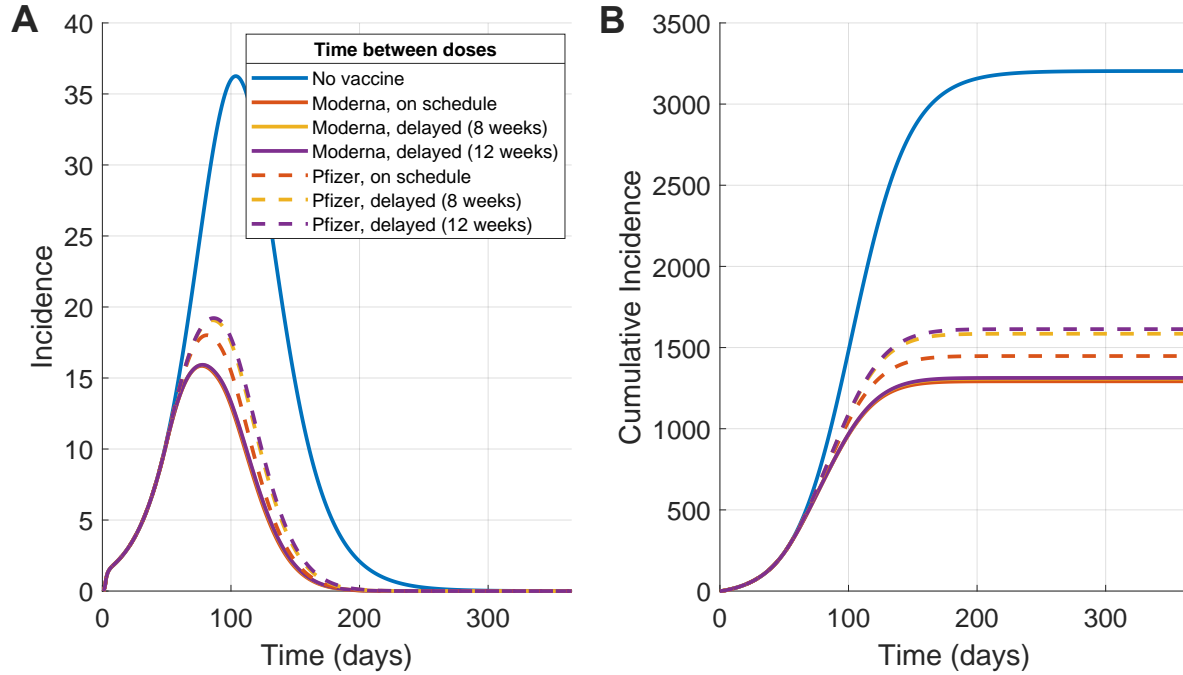
Figure 4.5: Incidence (A) and cumulative incidence (B) of the original variant, with 10% pre-existing immunity, and vaccines administered to the population.

Figure 4.4 shows the resulting overall attack rate with varying vaccination coverage, and a fixed pre-existing immunity of 10%. It could be seen that in both vaccines, vaccinating even just 20% of the population with Moderna vaccines resulted in a significant reduction in the attack rate, leading to 6.4% attack rate for the original variant, 20.8% for the Alpha variant, and 27.3% for the Delta variant. With Pfizer-BioNTech vaccines, the attack rates for the original, Alpha, and Delta variants were 6.8%, 21.2%, and 27.4% respectively. However, variations in vaccine escape do not result in a large difference in attack rates generated.

Assuming 20% of the population was fully-vaccinated with Moderna vaccines, for example, resulted to an overall herd immunity of 35.6% for the original variant, 50.4% for the Alpha variant, and 54.7% for the Delta variant. Meanwhile, with Pfizer-BioNTech vaccines, the resulting herd immunity was 34.0% for the original variant, 49.0% for the Alpha variant, and 54.4% for the Delta variant. These values were still lower than what would be obtained using homogeneous assumptions, in line with what was observed in Section 4.3.1.
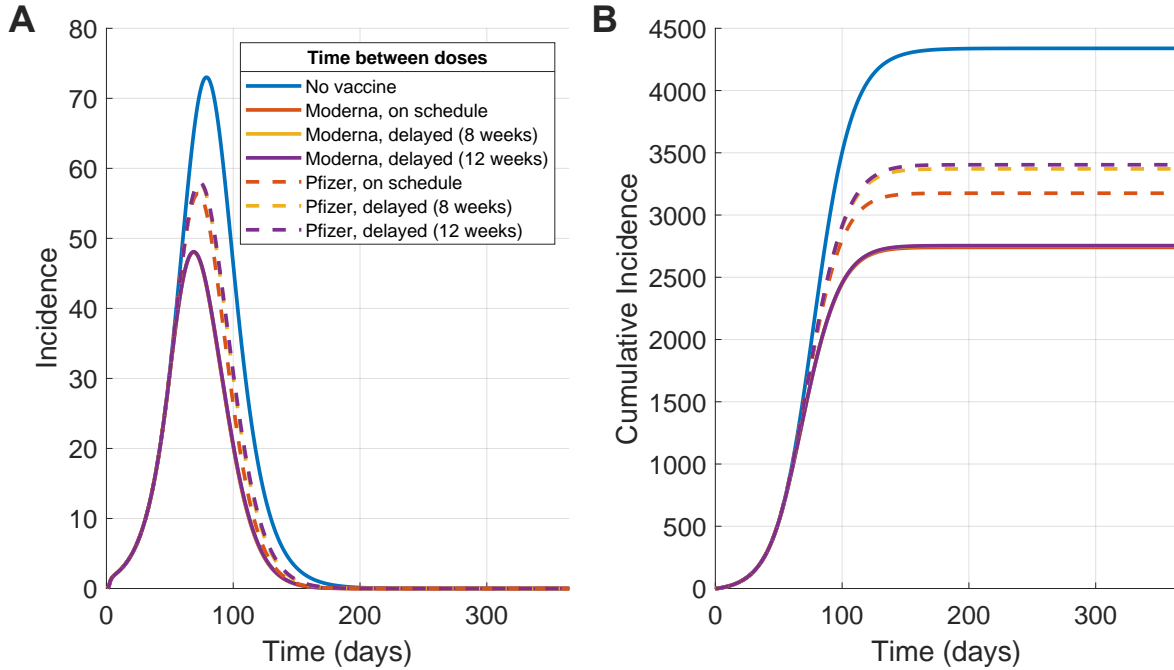
Figure 4.6: Incidence (A) and cumulative incidence (B) of the Alpha variant, with 10% pre-existing immunity, and vaccines administered to the population.

Figure 4.5 shows the effect of administering the Moderna and Pfizer-BioNTech vaccines to eligible age groups in the population with the original variant being the source of infection, and varying timelines between the two doses. Owing to the high vaccine efficacy against infection, vaccinating the population with Moderna vaccines reduced the total incidence by 59.0–59.7% compared to without vaccines; with Pfizer-BioNTech vaccines, 49.6–54.8% of the total incidence without vaccination was reduced. When changing the time between doses, the effect was more pronounced with the Pfizer-BioNTech vaccines than with Moderna vaccines. One reason for this is the higher efficacy of Moderna vaccines compared to Pfizer-BioNTech vaccines. Another reason could be that the recommended schedule between doses for Pfizer-BioNTech vaccines is 3 weeks; delaying the second dose to 8 weeks extends the duration of susceptibility of the population vaccinated with the first dose to infection. Figure 4.6 shows a similar trend, albeit less pronounced, in the reduction of total incidence with the Alpha variant. The obtained total incidences with Moderna and Pfizer-BioNTech vaccines were
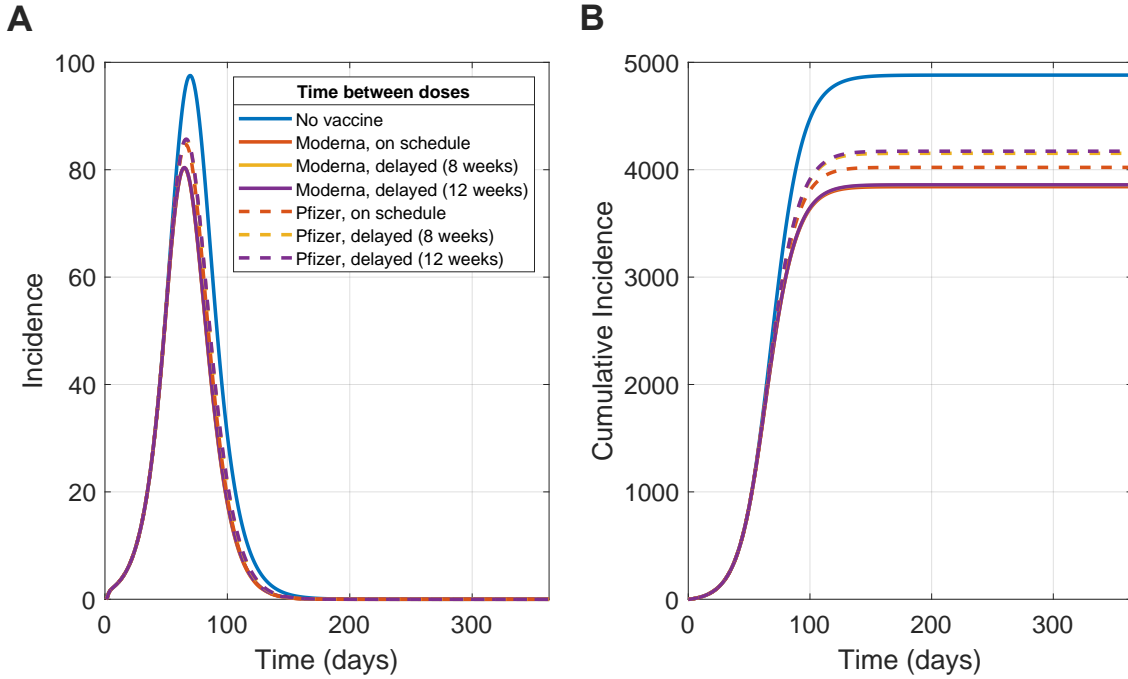
Figure 4.7: Incidence (A) and cumulative incidence (B) of the Delta variant, with 10% pre-existing immunity and 20% reduction in vaccine effectiveness.

63.2–63.5% and 73.2–78.5% of the total incidence with no vaccines respectively, due to the lower vaccine efficacy against infection compared with the original variant.

With the Delta variant, the different degrees of vaccine escape influence the effect of vaccination on the total incidence. While the total incidence still decreased significantly compared to no vaccine scenario, the effect of delaying the second dose becomes less pronounced as the vaccine escape increases. Figures 4.7-4.9 show that there is little change in the total incidence. Meanwhile, Pfizer-BioNTech still has a considerable difference between administering doses on-time and delaying to 8 weeks.

The effect of vaccination on the epidemic dynamics with multiple variants was also considered. Here, the Delta variant was introduced in the population 120 days after the start of simulation, where the first prevailing variant was Alpha. In comparing the incidence peaks for Alpha and Delta infections (Figures 4.10-4.15), we observed that Delta generated more

Figure 4.8: Incidence (A) and cumulative incidence (B) of the Delta variant, with 10% pre-existing immunity and 50% reduction in vaccine effectiveness.

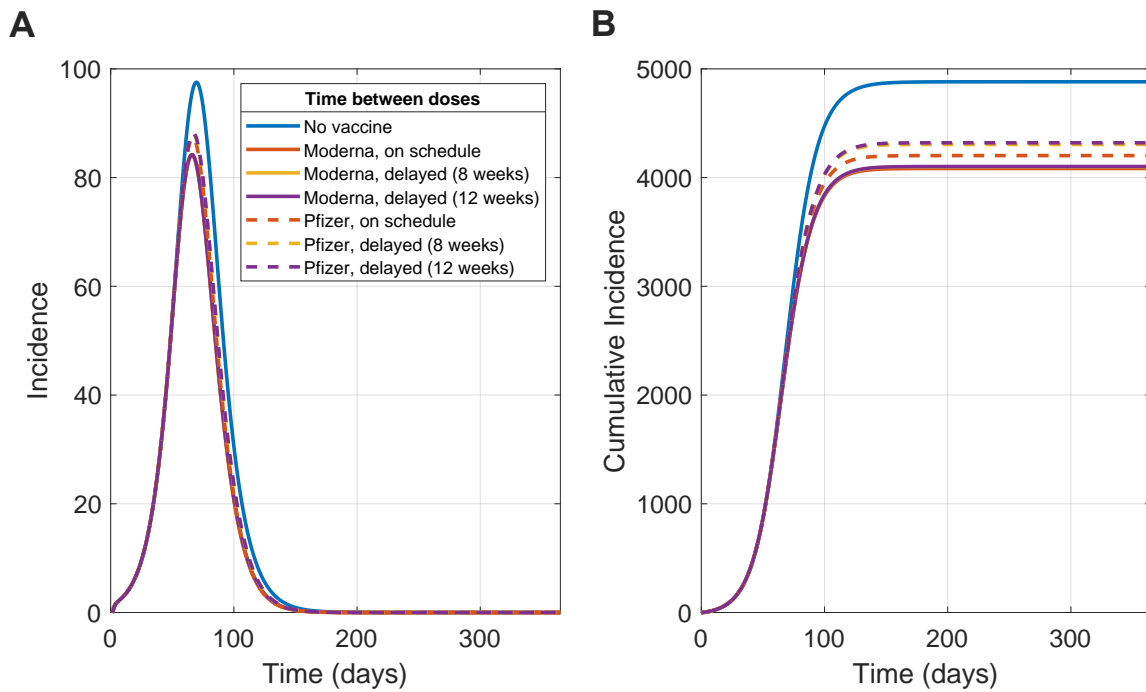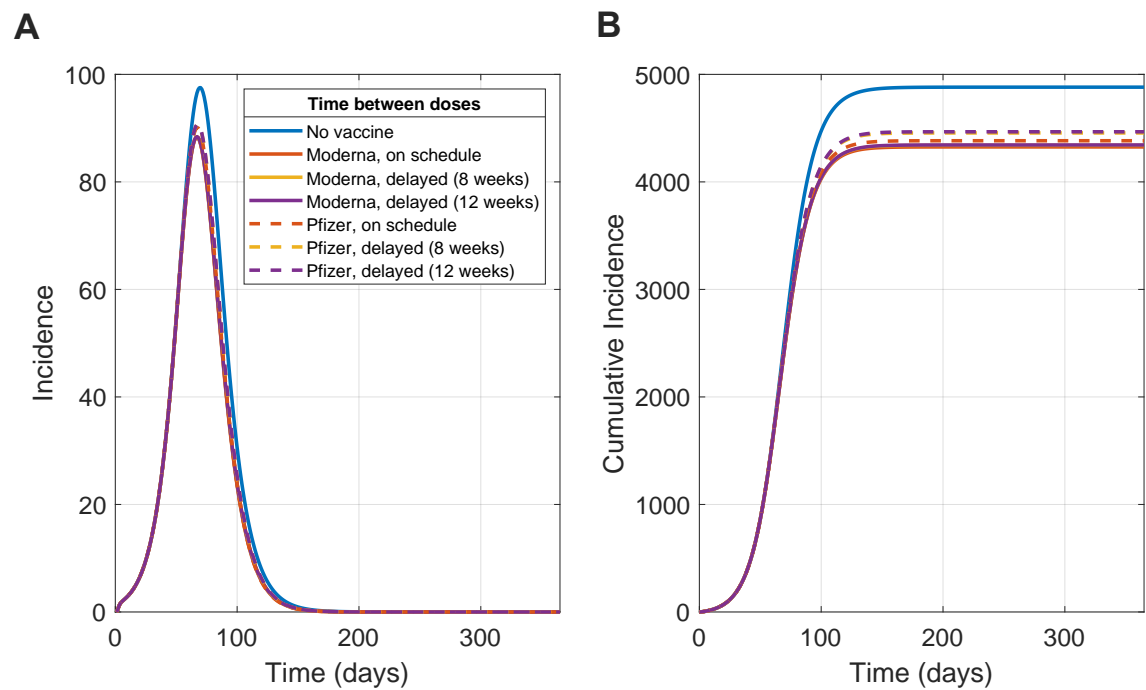

Figure 4.9: Incidence (A) and cumulative incidence (B) of the Delta variant, with 10% pre-existing immunity and 80% reduction in vaccine effectiveness.

infections due to its higher transmissibility, in addition to having a shorter time period for generation of new infections compared to Alpha. This is evidenced by the steeper increase for cumulative incidence for Delta compared to Alpha, which occurs for all the vaccine scenarios explored.

Compared with delivering vaccines on schedule, delaying the Moderna vaccine second dose by 8 weeks resulted in 120 more infections when there is 20% reduction of vaccine effectiveness (Figure 4.10-D), 116 more infections with 50% reduction in vaccine effectiveness (Figure 4.11-D), and 110 more infections with 80% reduction in vaccine effectiveness (Figure 4.12-D). With 12 weeks between doses, these values increased from the 8-week values by 50-60 more infections (Figures 4.10-F, 4.11-F, 4.12-F). For the Pfizer-BioNTech vaccines, an 8-week delay between doses caused an increase of 371 cases when there is 20% reduction in vaccine effectiveness (Figure 4.13-D), 223 cases with 50% reduction in vaccine effectiveness (Figure 4.14-D), and 95 cases with 80% reduction in vaccine effectiveness (Figure 4.15-D) as compared to on schedule 3-week time-interval between doses. A longer delay of 12 weeks caused an additional 90 to 264 infections from the 8-week values (Figures 4.13-F, 4.14-F, 4.15-F). For scenarios dealing with only the Delta variant, the greatest influence of delaying the second dose of the vaccine occurs with the lowest reduction in vaccine effectiveness, with the Pfizer-BioNTech vaccines having a more significant difference in outcomes than Moderna vaccines.

4.3.4 Effect of re-infection

As expected, introducing re-infection to the model would result in a second peak in incidence corresponding to secondary infections (Figure 4.16), which is smaller than the peak corresponding to primary infections. The timing of these peaks depends on the transmissibility of infection, as well as the average duration of protection conferred by primary infection. For

Figure 4.10: Incidence and cumulative incidence graphs for Scenario 4.1 (Alpha and Delta, with 10% pre-existing immunity and 20% reduction of vaccine effectiveness), with Moderna vaccines administered on schedule (A, B) and with delays of 8 weeks (C, D) and 12 weeks (E, F) between doses.

Figure 4.11: Incidence and cumulative incidence graphs for Scenario 4.2 (Alpha and Delta, with 10% pre-existing immunity and 50% reduction of vaccine effectiveness), with Moderna vaccines administered on schedule (A, B) and with delays of 8 weeks (C, D) and 12 weeks (E, F) between doses.
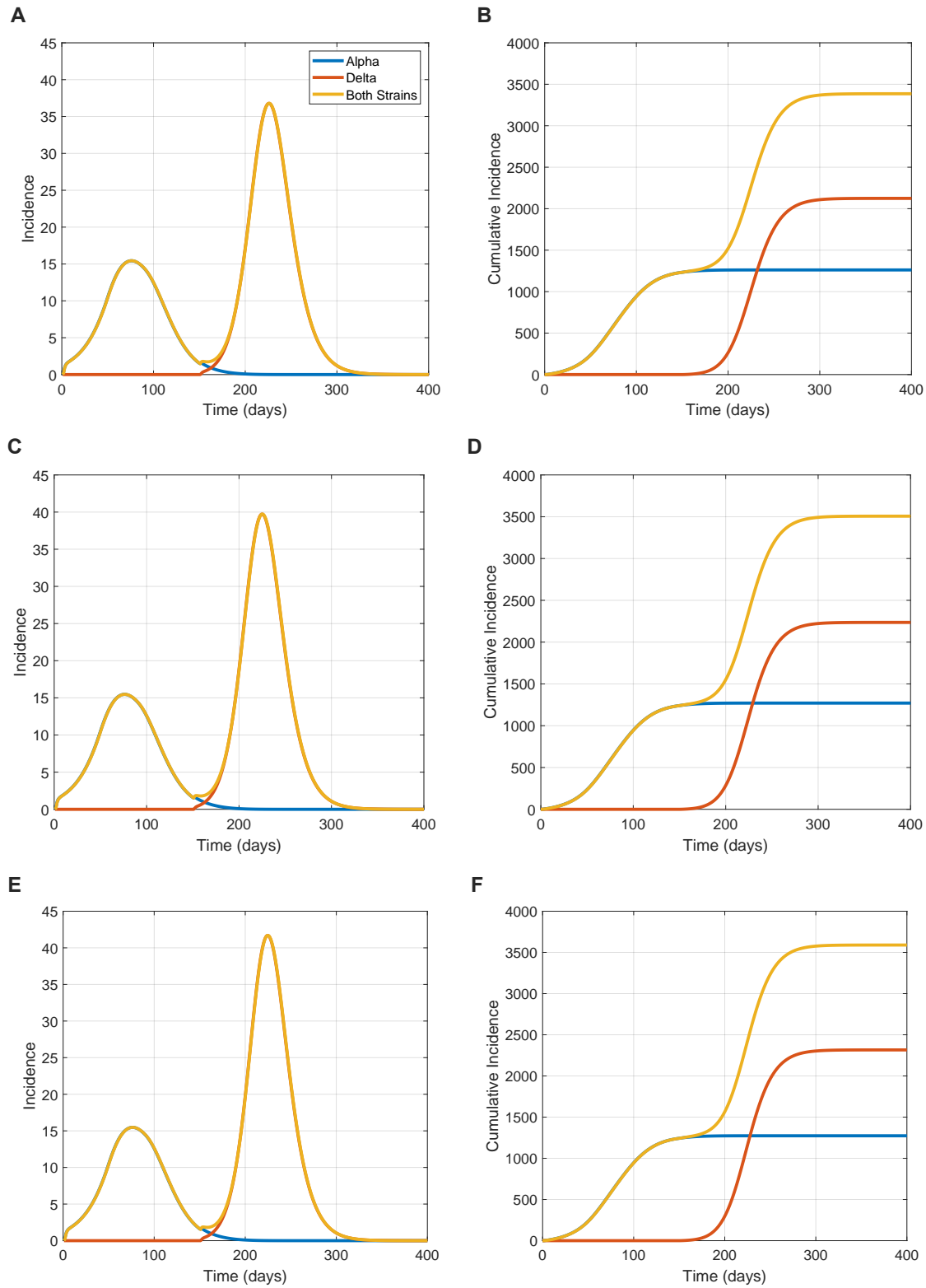
Figure 4.12: Incidence and cumulative incidence graphs for Scenario 4.3 (Alpha and Delta, with 10% pre-existing immunity and 80% reduction of vaccine effectiveness), with Moderna vaccines administered on schedule (A, B) and with delays of 8 weeks (C, D) and 12 weeks (E, F) between doses.
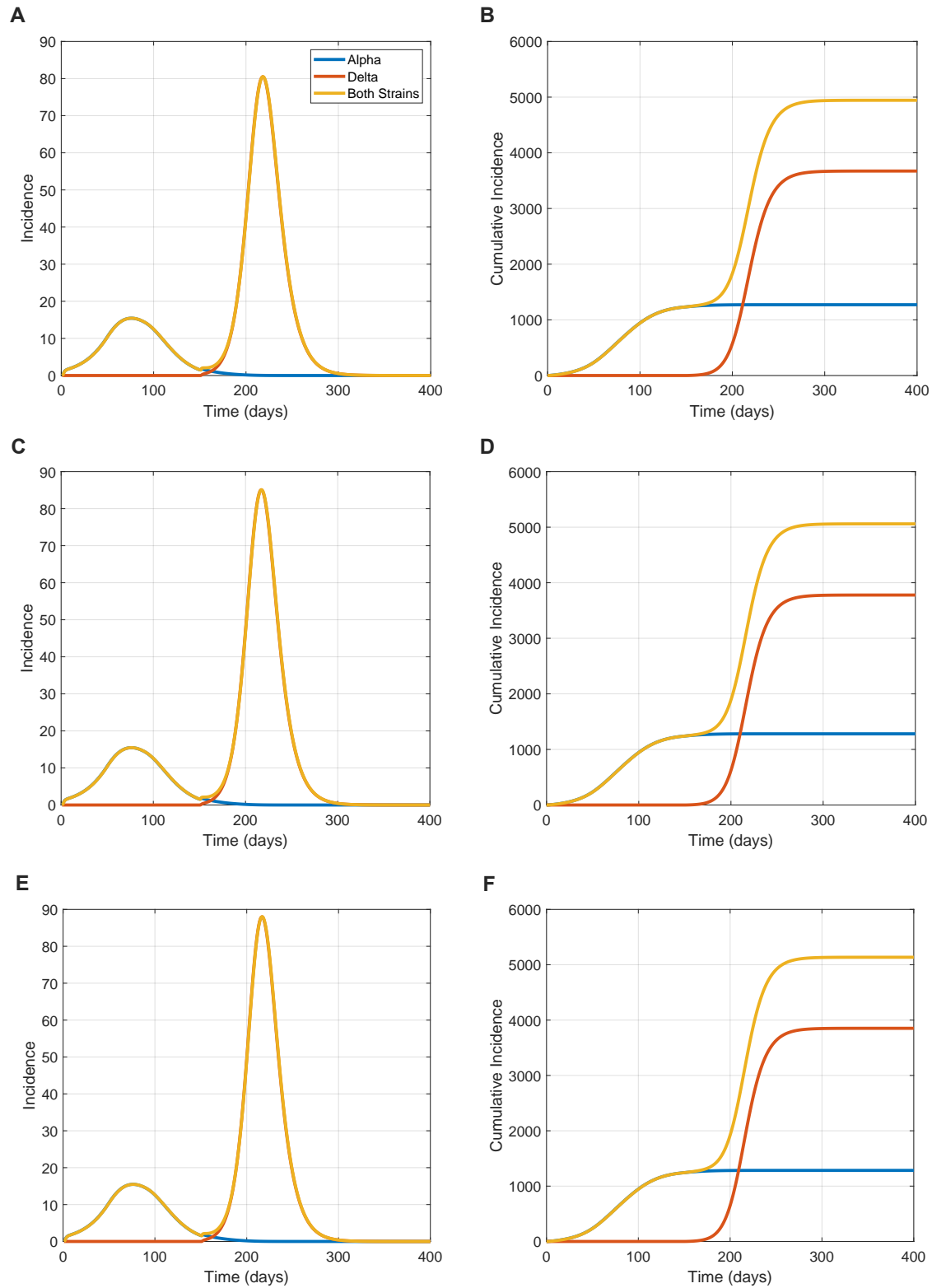
46

Figure 4.13: Incidence and cumulative incidence graphs for Scenario 4.1 (Alpha and Delta, with 10% pre-existing immunity and 20% reduction of vaccine effectiveness), with Pfizer-BioNTech vaccines administered on schedule (A, B) and with delays of 8 weeks (C, D) and 12 weeks (E, F) between doses.

Figure 4.14: Incidence and cumulative incidence graphs for Scenario 4.2 (Alpha and Delta, with 10% pre-existing immunity and 50% reduction of vaccine effectiveness), with Pfizer-BioNTech vaccines administered on schedule (A, B) and with delays of 8 weeks (C, D) and 12 weeks (E, F) between doses.
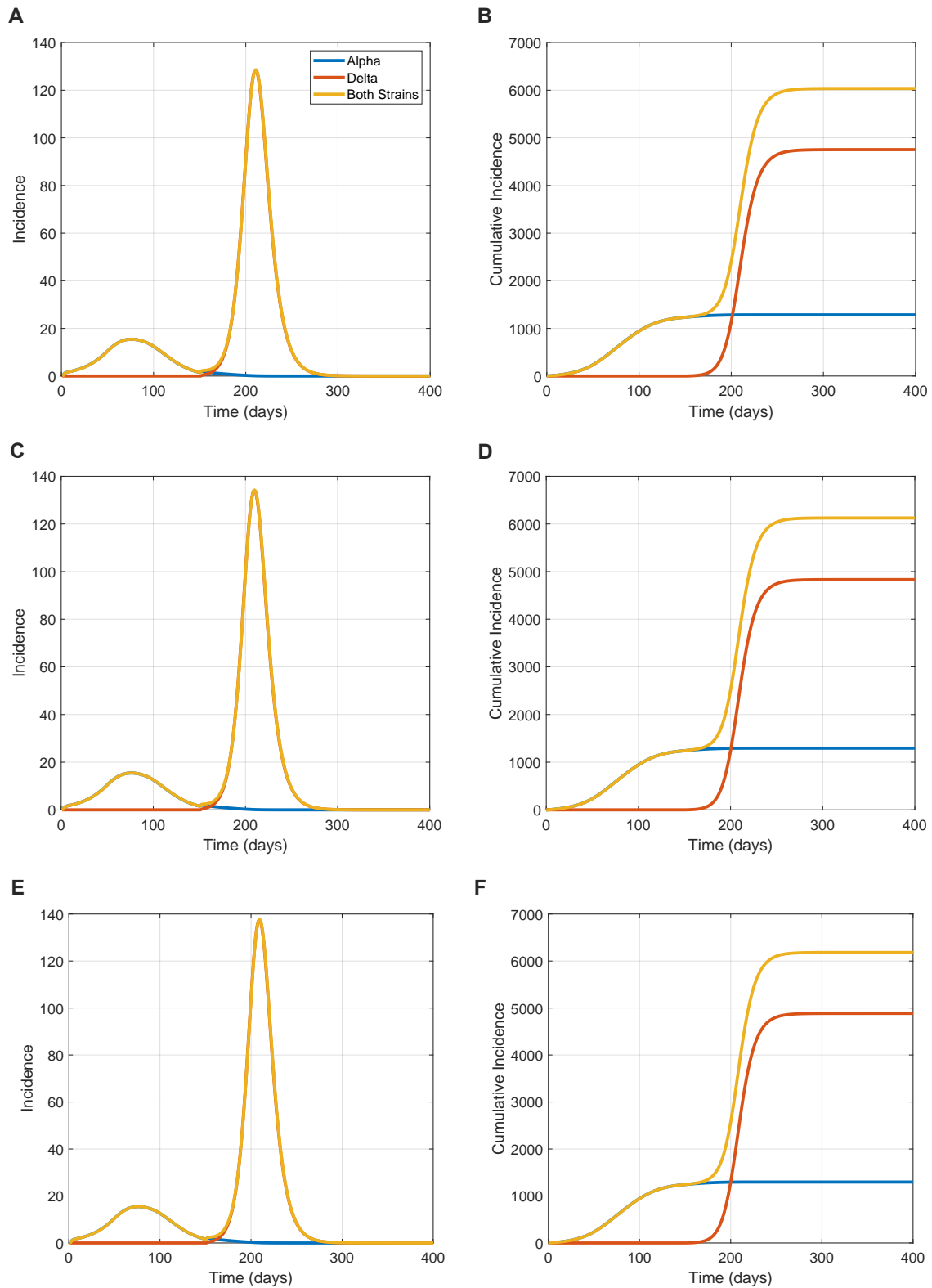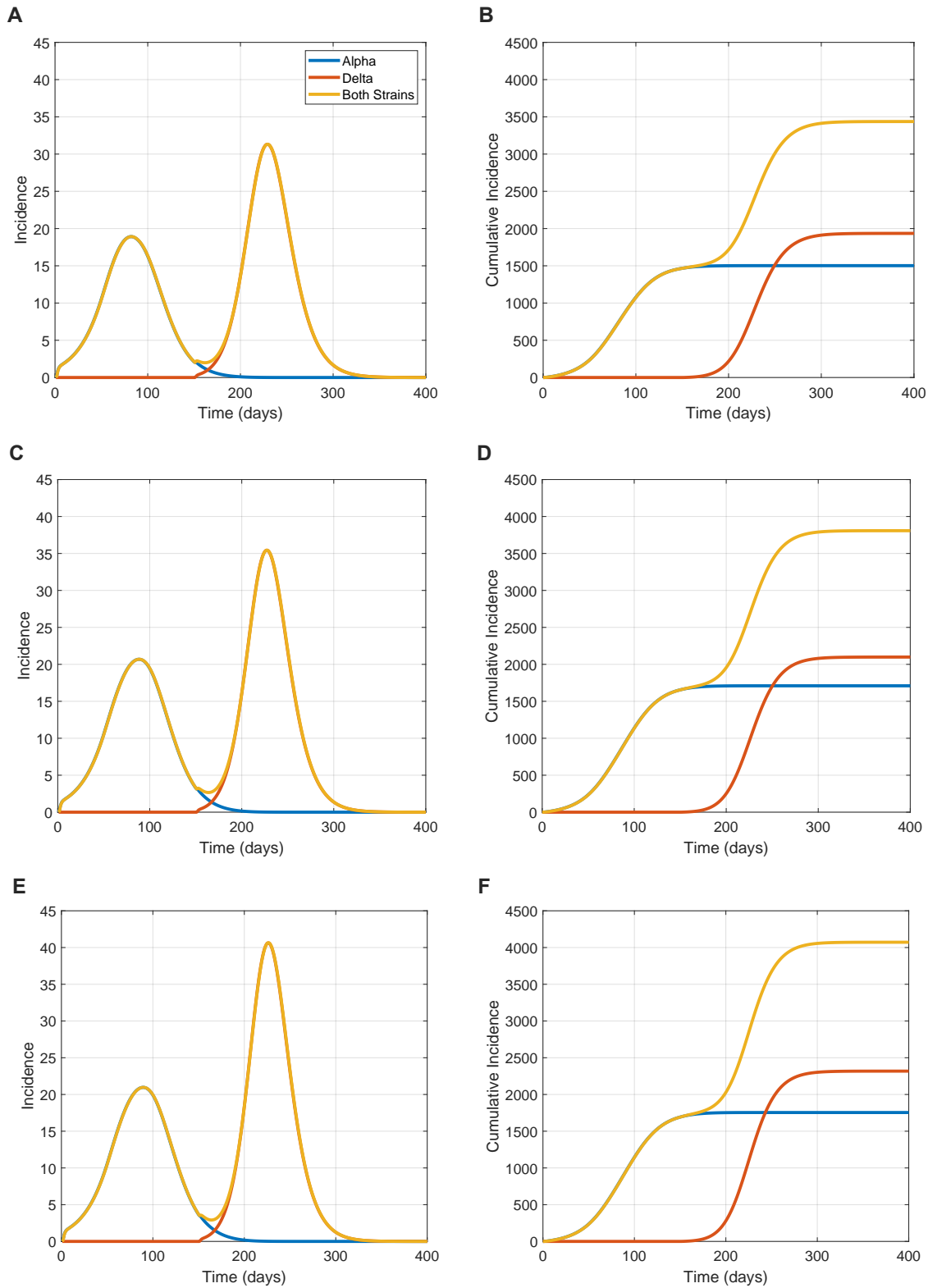
Figure 4.15: Incidence and cumulative incidence graphs for Scenario 4.3 (Alpha and Delta, with 10% pre-existing immunity and 80% reduction of vaccine effectiveness), with Pfizer-BioNTech vaccines administered on schedule (A, B) and with delays of 8 weeks (C, D) and 12 weeks (E, F) between doses.
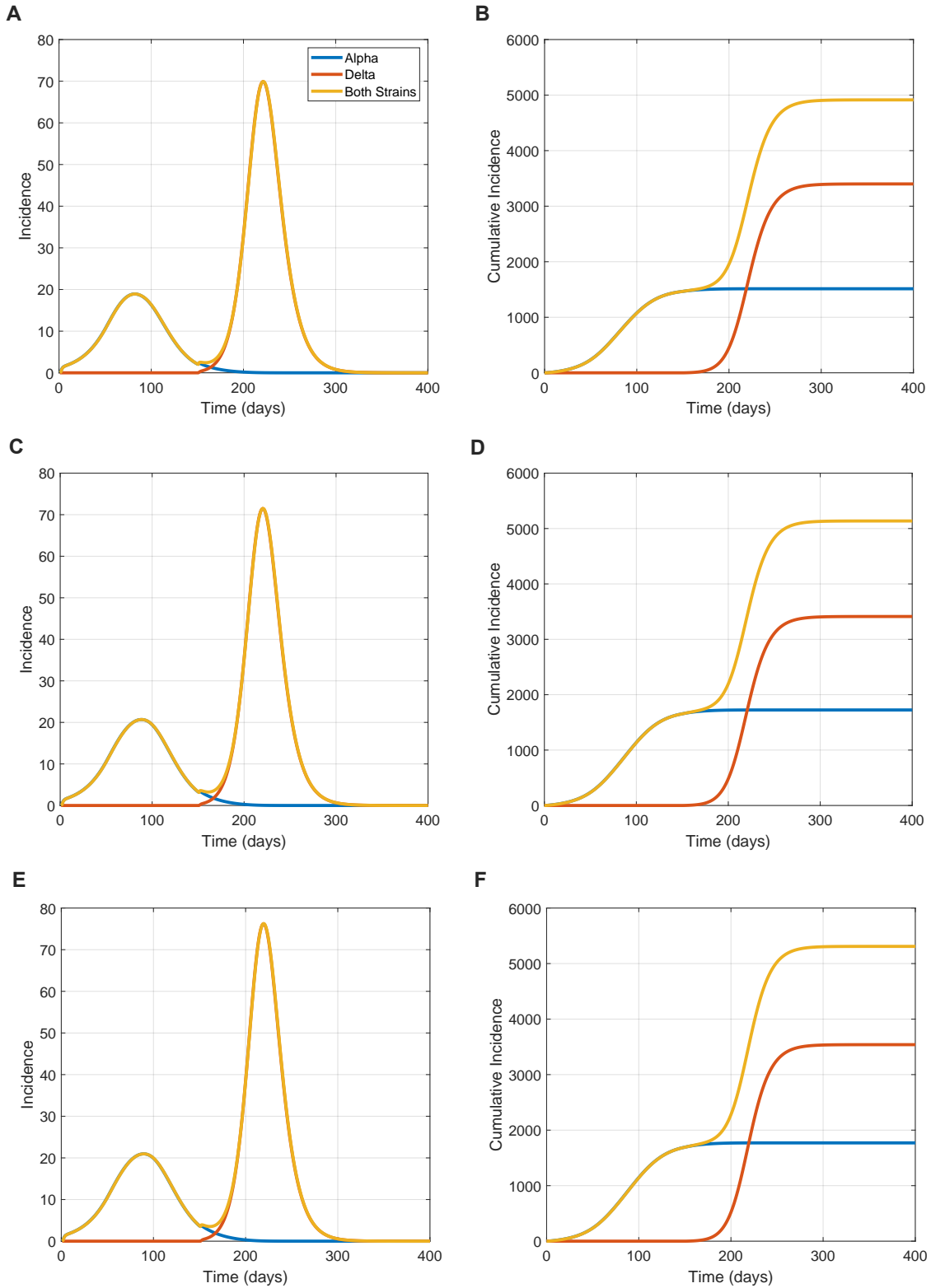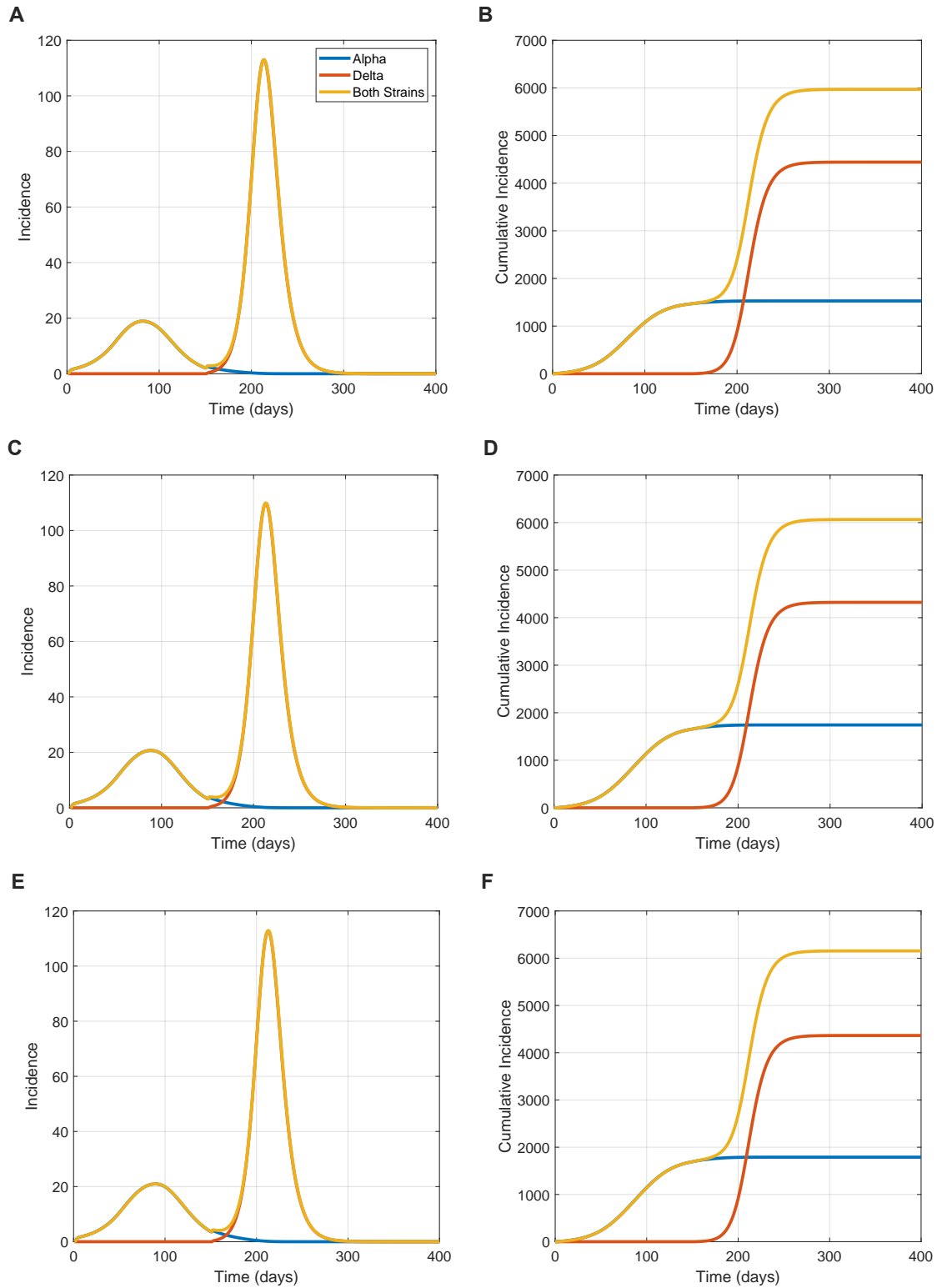
a given average duration of protection, increasing the transmissibility results in a shorter time interval between peaks. On the other hand, fixing the variant involved, increasing the average duration of protection delays the second peak, as well as a period between peaks in which incidence is relatively low.

A similar trend can be observed in the case of multiple variants with no control measures implemented (Scenario 4.0). Figures 4.17-4.20 show that with the introduction of the more transmissible Delta variant into the population, the Alpha variant is out-competed and therefore does not cause re-infection. With shorter duration of protection (Figures 4.17 and 4.18), there is still a short period where Alpha re-infections occur, but does not lead to another peak. In this case, the third peak is solely caused by Delta infections.

Figures 4.21 and 4.22 show the comparison between identifying and isolating asymptomatic and pre-symptomatic individuals in the absence of vaccination, while varying the average duration of protection. For these cases, increasing the average duration of protection allows for a delayed appearance of re-infection peaks, similar to what was observed with no control measures. However, a noticeable difference lies in the number of incidence peaks generated within the two-year span. It could be seen that for the asymptomatic case, even though the peak heights decrease with increasing identification, there are still three peaks generated within the same time frame, corresponding to Alpha, Delta, and secondary Delta infections.

On the other hand, in isolating pre-symptomatic individuals, the Alpha peaks die down with increasing identification. However, this does not prevent Delta infections from occurring, and oscillations in incidence are still observed. Identifying and isolating a larger proportion of Alpha infections in the pre-symptomatic stage comprises 53.3% to 80.3% of the infected population (see Table 3.4). In the absence of vaccination, and with infection being the only contributor to the rise of herd immunity, this causes a decreased chance of generating herd immunity while the Alpha variant is still dominant. Thus, with the introduction of the more transmissible Delta variant, susceptibility of the population is still high, leading a larger
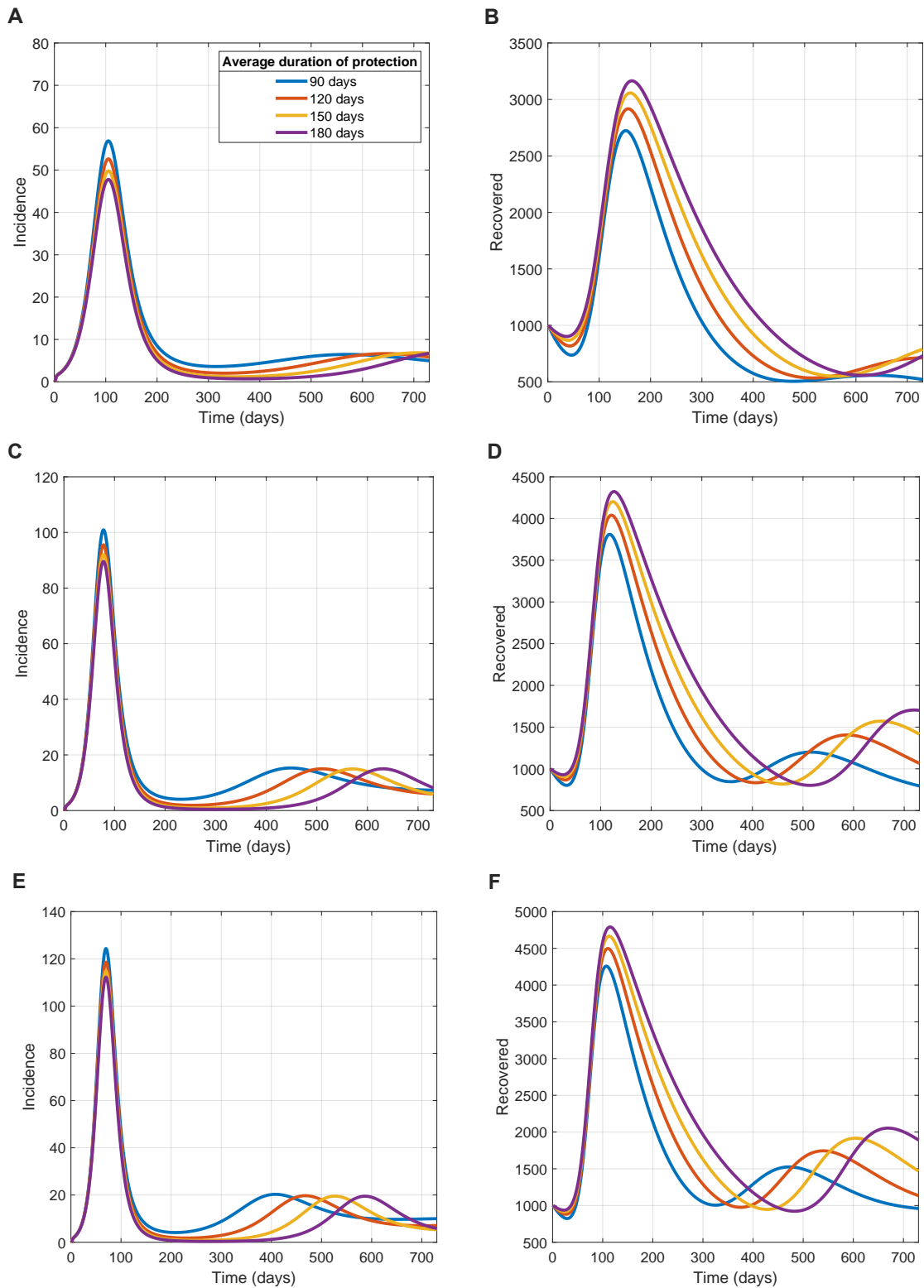
Figure 4.16: Incidence and total recovered of original variant (A, B), Alpha variant (C, D), and Delta variant (E, F), with 10% pre-existing immunity, no control measures, and varying average duration of protection.

Figure 4.17: Incidence (A) and total recovered (B) graphs for for Scenario 4.0 (Alpha and Delta, with 10% pre-existing immunity and no control measures introduced), and an average of 90 days for duration of protection after recovery from infection.
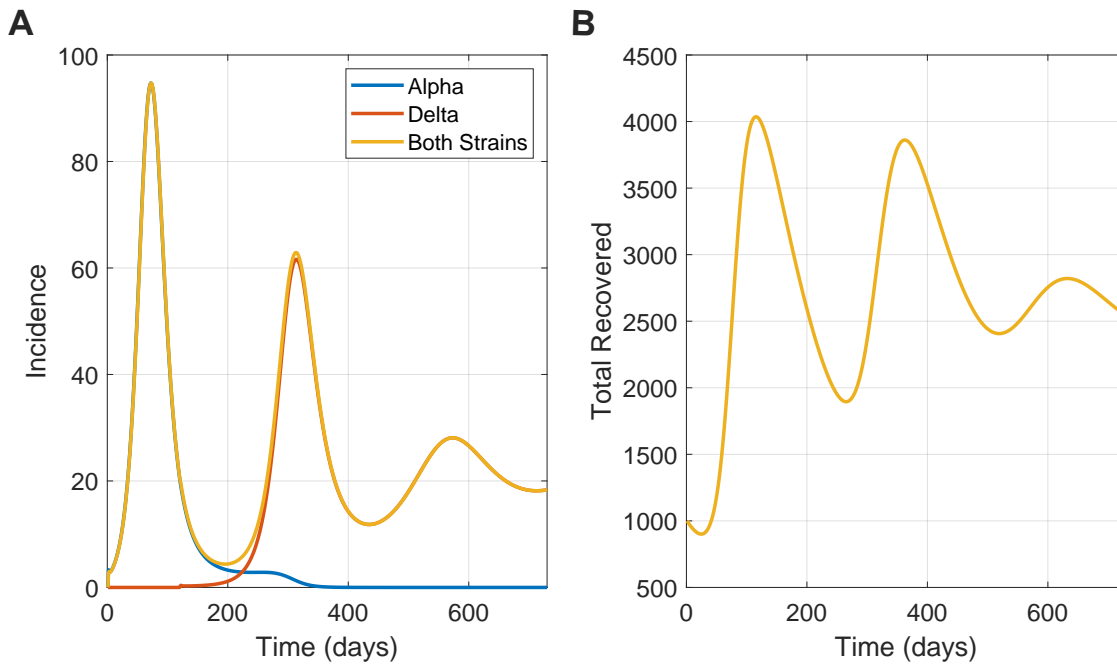
Figure 4.18: Incidence (A) and total recovered (B) graphs for for Scenario 4.0 (Alpha and Delta, with 10% pre-existing immunity and no control measures introduced), and an average of 120 days for duration of protection after recovery from infection.

Figure 4.19: Incidence (A) and total recovered (B) graphs for for Scenario 4.0 (Alpha and Delta, with 10% pre-existing immunity and no control measures introduced), and an average of 150 days for duration of protection after recovery from infection.

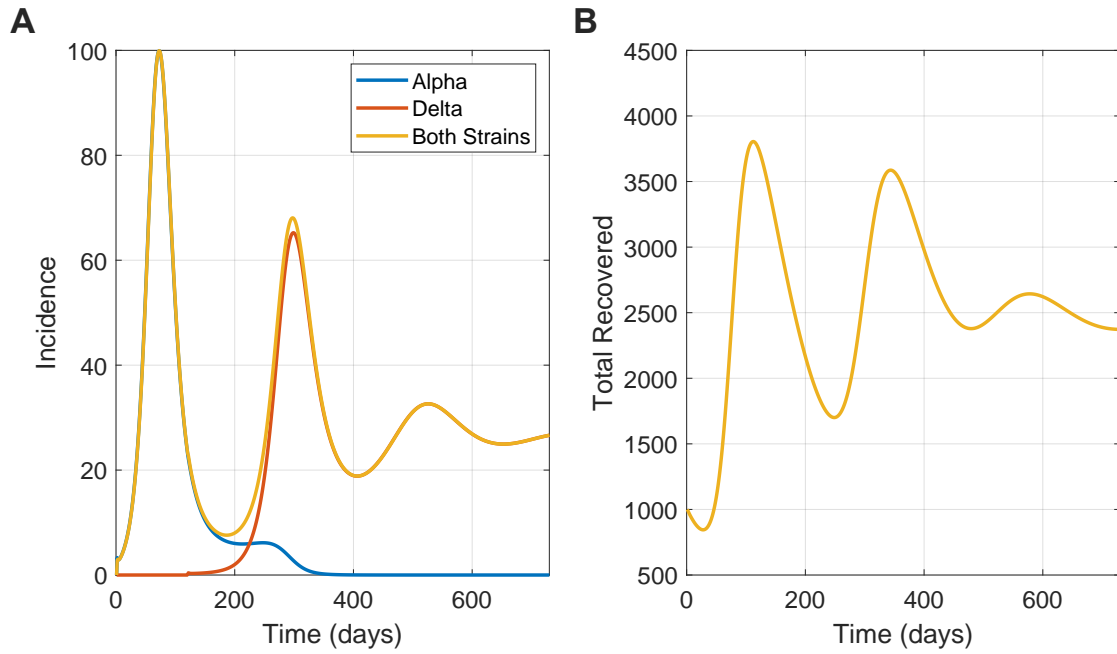**Figure 4.20:** Incidence (A) and total recovered (B) graphs for for Scenario 4.0 (Alpha and Delta, with 10% pre-existing immunity and no control measures introduced), and an average of 180 days for duration of protection after recovery from infection.
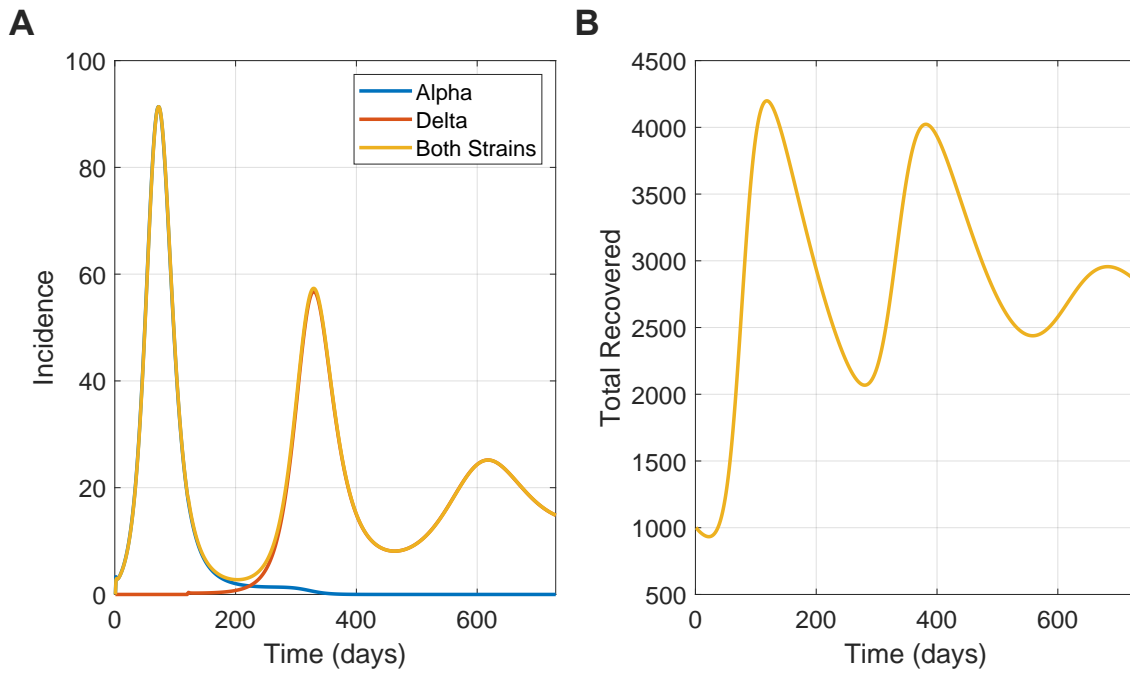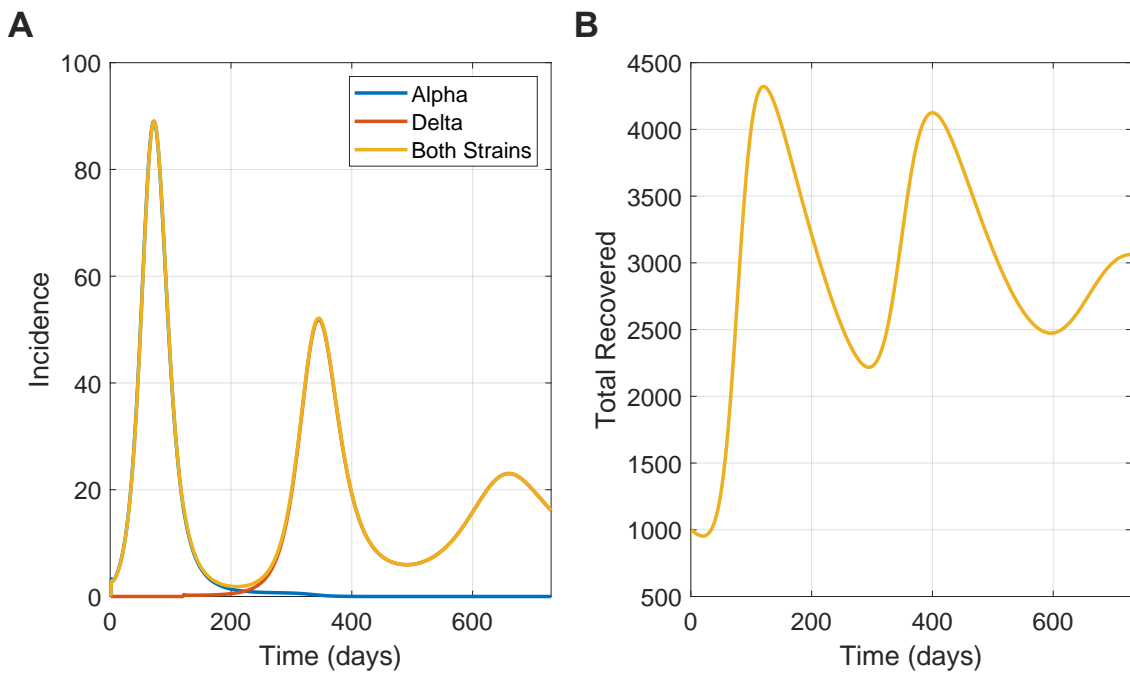
epidemic wave.

Lastly, the effect of vaccination (without identification and isolation) on re-infection with multiple variants was examined. Figures 4.23 to 4.26 illustrate the case wherein Moderna vaccines were administered on schedule, identification and isolation of infected individuals were not implemented, and vaccine effectiveness towards the Delta variant was reduced by 20% (Scenario 4.1), while Figures 4.27 to 4.30 show the case wherein Pfizer-BioNTech vaccines were used, with the rest of the conditions kept the same as the Moderna case. As with the previous re-infection scenarios, the average duration of protection after recovery from infection was varied from 90 days to 180 days.

Similar to the scenario with no control measures (S4.0), the third peak corresponds to re-infections generated solely by the Delta variant. As with the case of no re-infection, vaccination lowers the peak incidence over the course of the epidemic. However, it could also be seen that vaccination delays the appearance of the third peak, which is further amplified by increasing the average duration of protection. This is observed for both Moderna and Pfizer-BioNTech vaccines.

As a concluding remark for the results observed here, we note that while waning immunity causes a decrease in herd immunity, the potential for re-infection allows for herd immunity to build up again, leading to oscillatory behaviour. However, the epidemic will not become extinct regardless of the variant characteristics, identification and isolation of cases, or vaccine scenarios, but rather will reach a steady state over time.
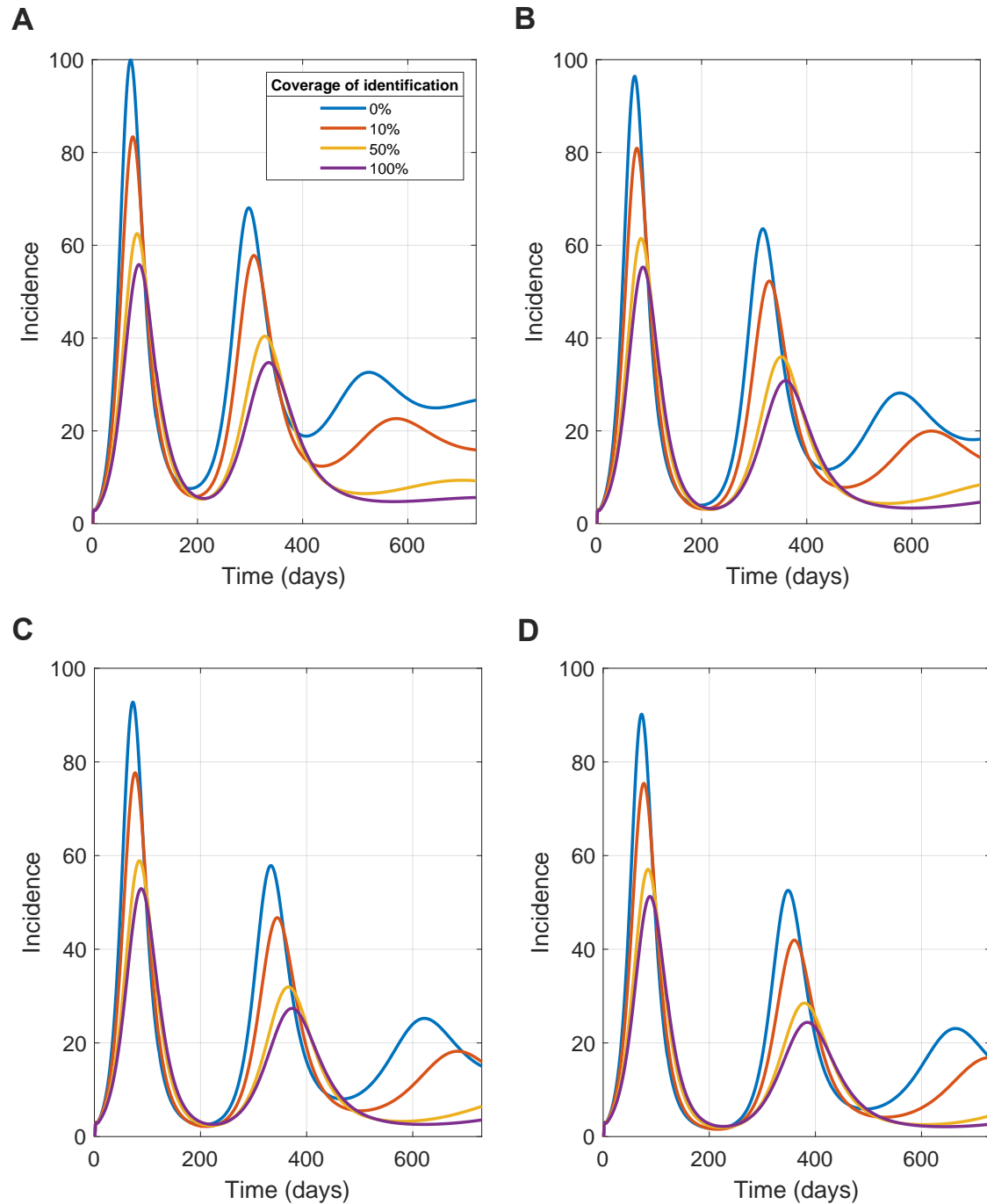
Figure 4.21: Total incidence graphs for Scenario 4.0 (Alpha and Delta, with 10% pre-existing immunity and no vaccines introduced), with identification of asymptomatic infections with a 2-day delay, and 90 days (A), 120 days (B), 150 days (C), and 180 days (D) average duration of protection after recovery from infection.
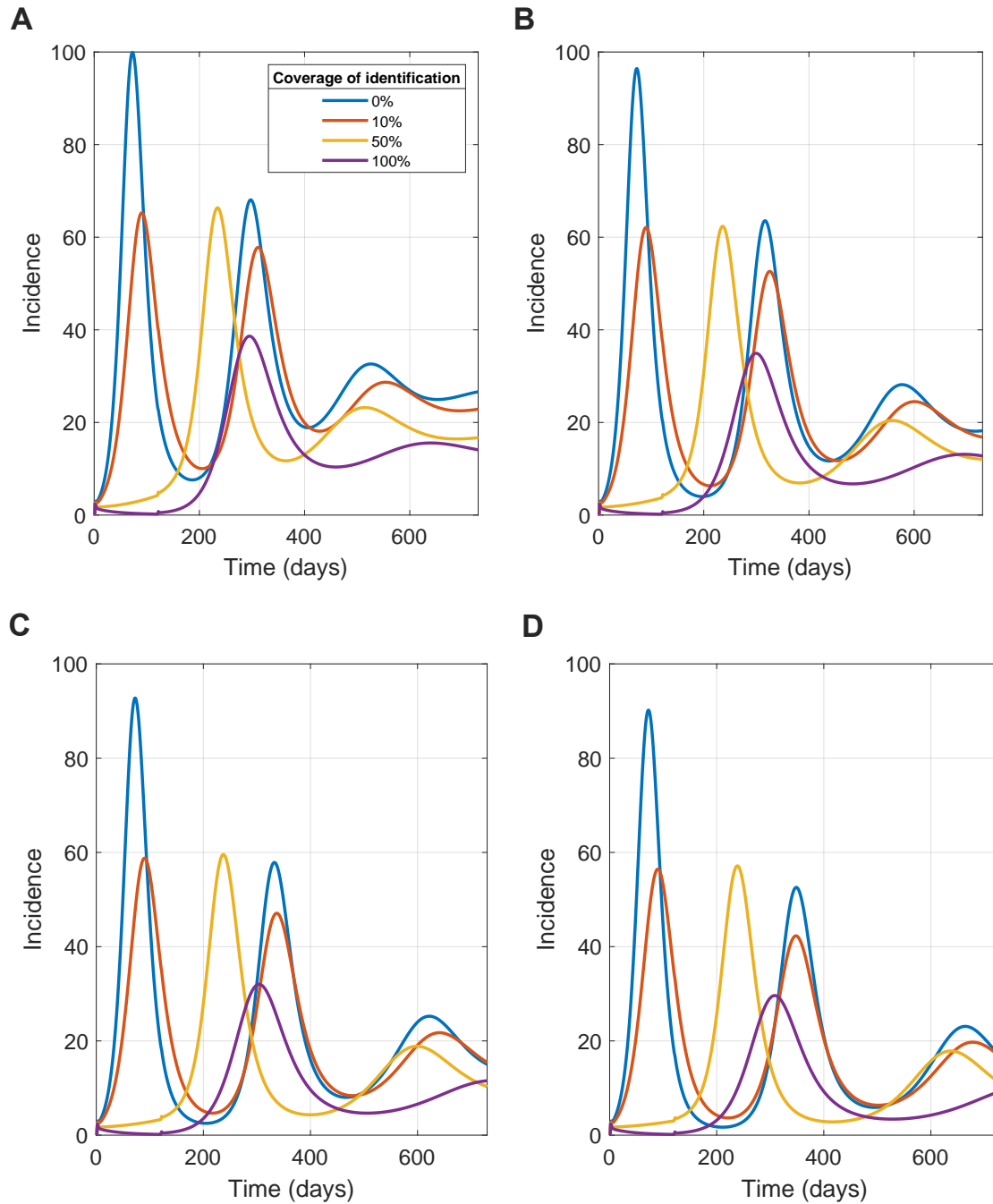
Figure 4.22: Total incidence graphs for Scenario 4.0 (Alpha and Delta, with 10% pre-existing immunity and no vaccines introduced), with identification of pre-symptomatic infections with a 2-day delay, and 90 days (A), 120 days (B), 150 days (C), and 180 days (D) average duration of protection after recovery from infection.

Figure 4.23: Incidence (A) and total recovered (B) graphs for Scenario 4.1 (Alpha and Delta, with 10% pre-existing immunity and 20% reduction of vaccine effectiveness), with Moderna vaccine administered on schedule, and an average of 90 days for duration of protection after recovery from infection.

Figure 4.24: Incidence (A) and total recovered (B) graphs for Scenario 4.1 (Alpha and Delta, with 10% pre-existing immunity and 20% reduction of vaccine effectiveness), with Moderna vaccine administered on schedule, and an average of 120 days for duration of protection after recovery from infection.

Figure 4.25: Incidence (A) and total recovered (B) graphs for Scenario 4.1 (Alpha and Delta, with 10% pre-existing immunity and 20% reduction of vaccine effectiveness), with Moderna vaccine administered on schedule, and an average of 150 days for duration of protection after recovery from infection.

Figure 4.26: Incidence (A) and total recovered (B) graphs for Scenario 4.1 (Alpha and Delta, with 10% pre-existing immunity and 20% reduction of vaccine effectiveness), with Moderna vaccine administered on schedule, and an average of 180 days for duration of protection after recovery from infection.

Figure 4.27: Incidence (A) and total recovered (B) graphs for Scenario 4.1 (Alpha and Delta, with 10% pre-existing immunity and 20% reduction of vaccine effectiveness), with Pfizer-BioNTech vaccine administered on schedule, and an average of 90 days for duration of protection after recovery from infection.
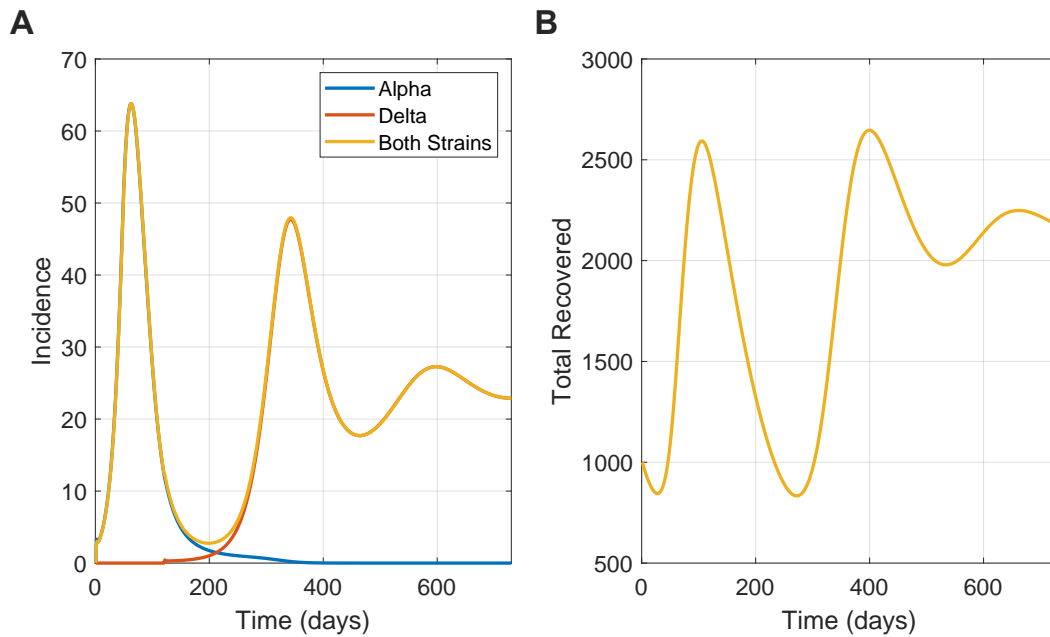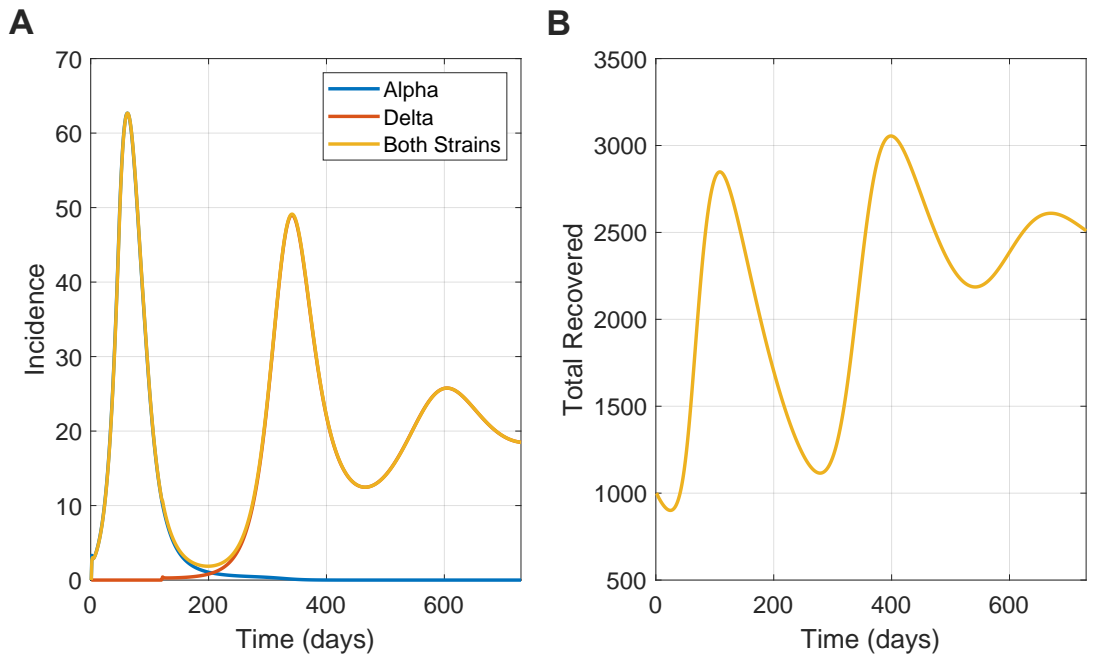

Figure 4.28: Incidence (A) and total recovered (B) graphs for Scenario 4.1 (Alpha and Delta, with 10% pre-existing immunity and 20% reduction of vaccine effectiveness), with Pfizer-BioNTech vaccine administered on schedule, and an average of 120 days for duration of protection after recovery from infection.
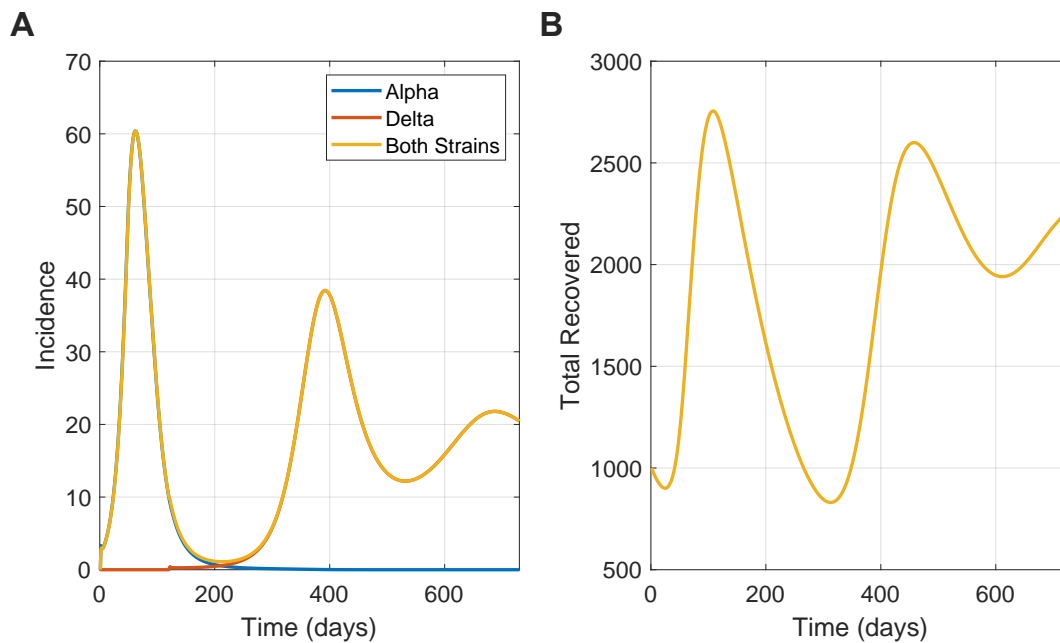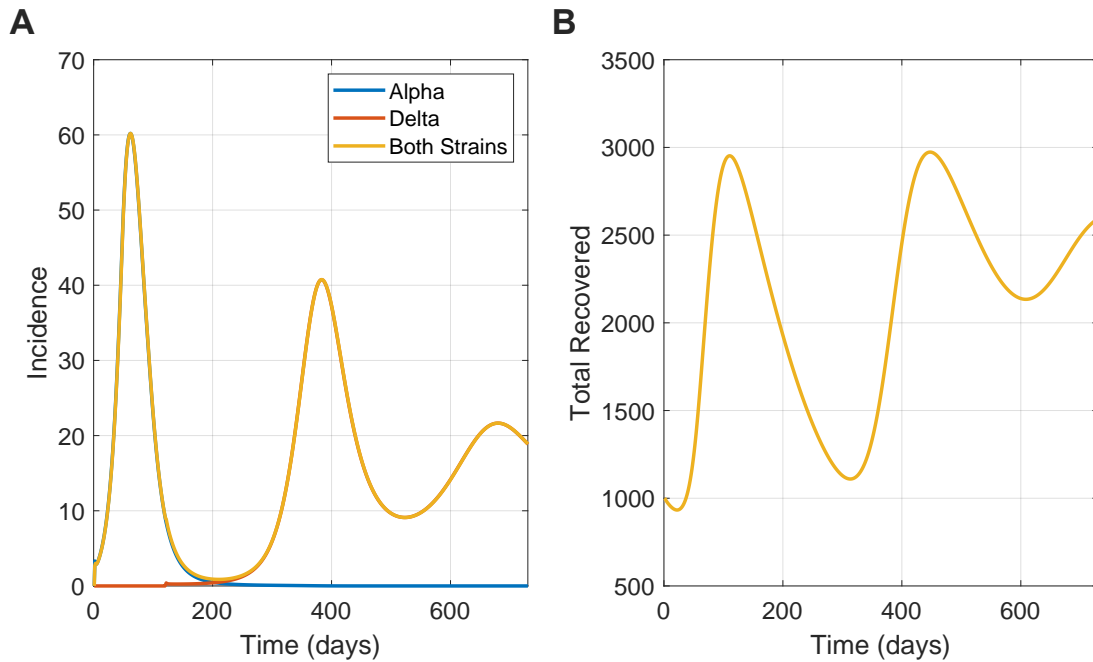
Figure 4.29: Incidence (A) and total recovered (B) graphs for Scenario 4.1 (Alpha and Delta, with 10% pre-existing immunity and 20% reduction of vaccine effectiveness), with Pfizer-BioNTech vaccine administered on schedule, and an average of 150 days for duration of protection after recovery from infection.
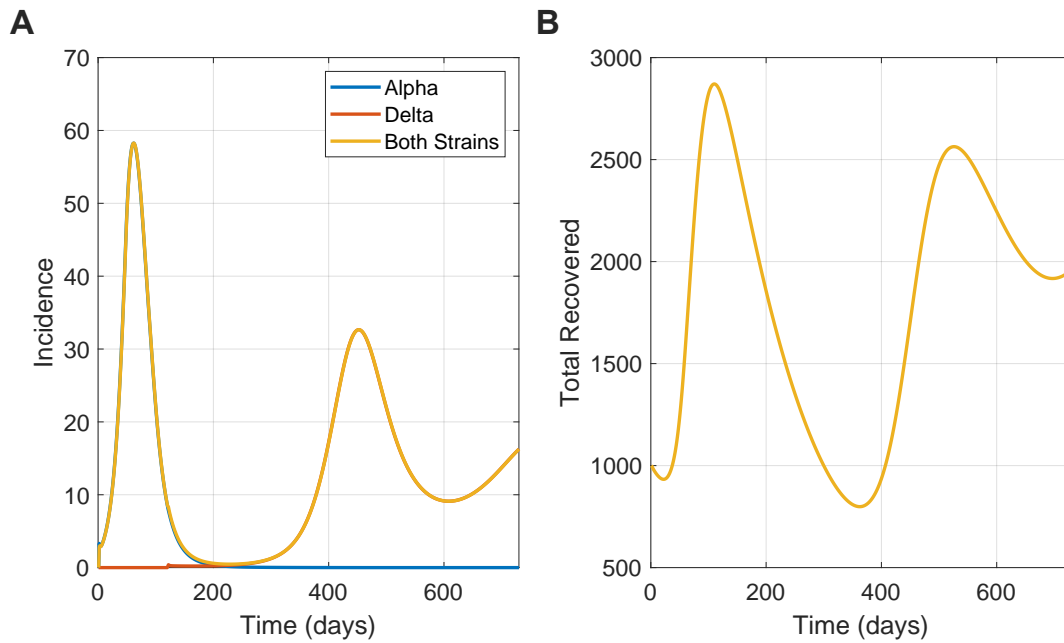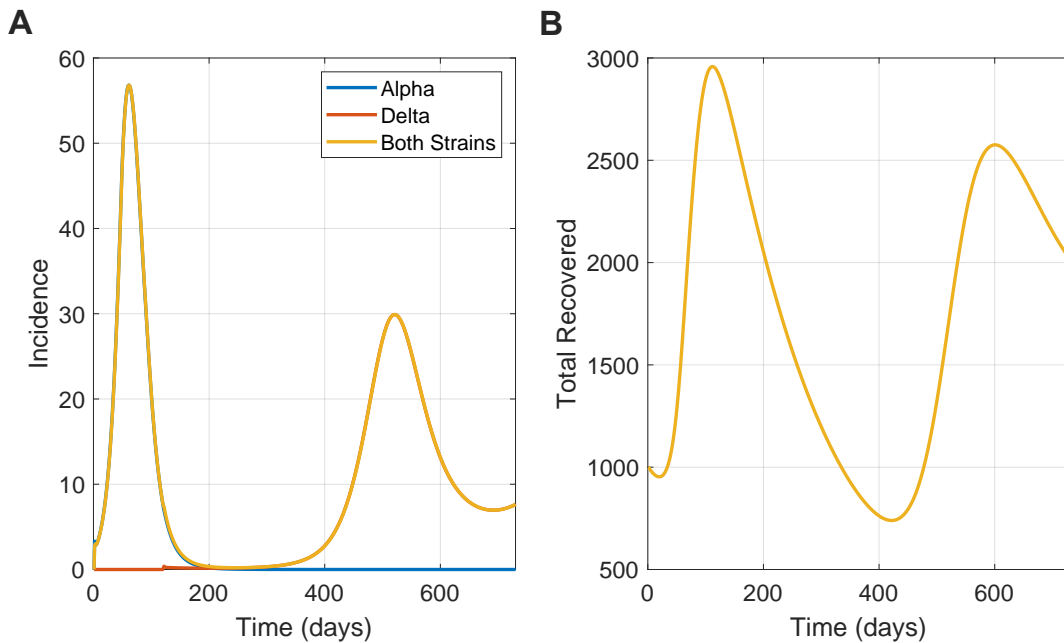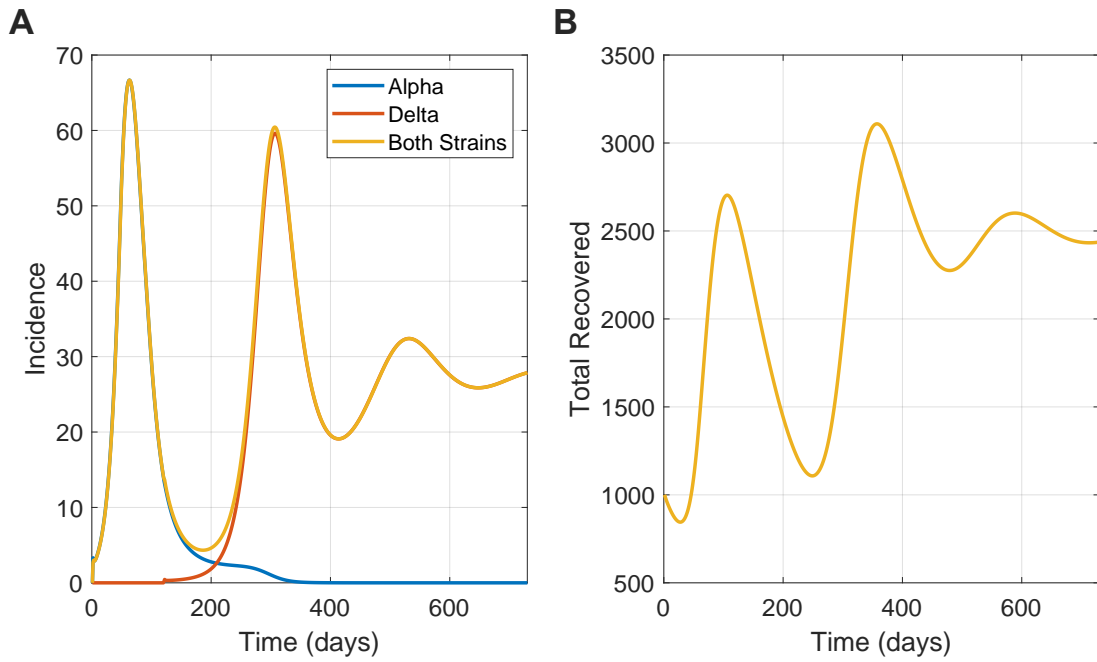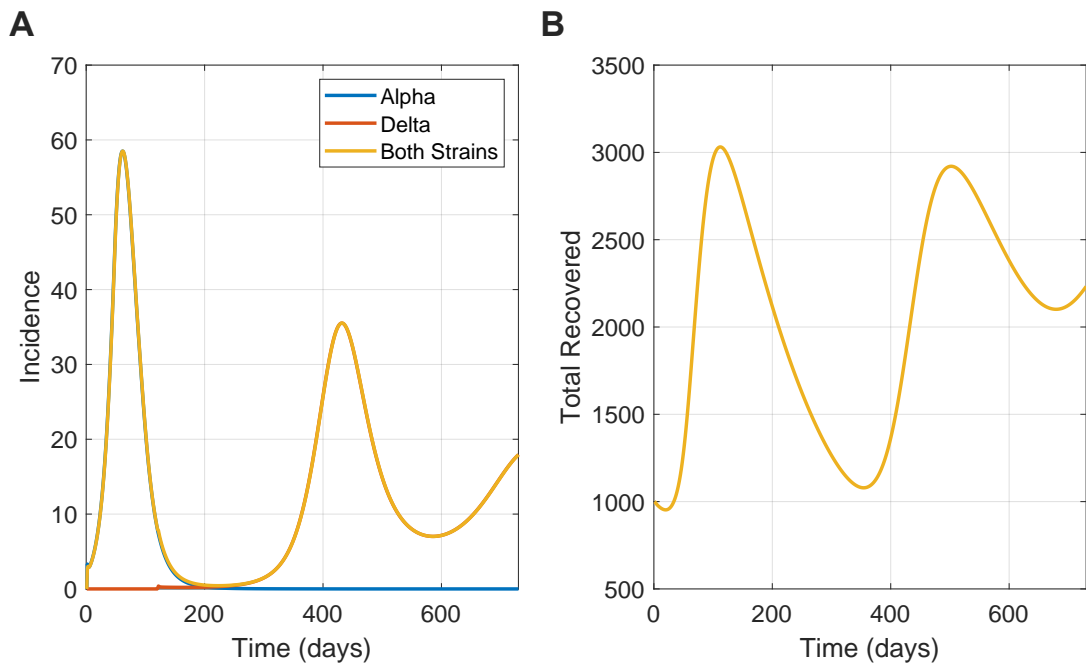

Figure 4.30: Incidence (A) and total recovered (B) graphs for Scenario 4.1 (Alpha and Delta, with 10% pre-existing immunity and 20% reduction of vaccine effectiveness), with Pfizer-BioNTech vaccine administered on schedule, and an average of 180 days for duration of protection after recovery from infection.

Chapter 5

Discussion

During the early stages of the COVID-19 pandemic, with only non-pharmaceutical inter-ventions available as prevention measures against further spread of disease, the goal in implementing these measures was to suppress the outbreaks, and reduce health burden. With the introduction of vaccines, although imperfect in conferring full protection against infection, several key questions have come up, such as the minimum vaccination coverage required for pandemic control, or which target demographic should be prioritised given limited vaccine supply. All of these in turn relate to the concept of achieving herd immunity. This thesis aimed to identify how heterogeneity in the population affects the herd immunity required to curtail an outbreak, and how control measures such as identification and isolation of infected individuals, and vaccination of susceptible individuals, influence the progression of the epidemic in the population, both in single- and multiple-variant infections, and with the case of transient protection and re-infection as observed recently.

The results of this thesis show that even in the absence of any control measures, and without any pre-existing immunity in the population, age and contact heterogeneity in the population are key drivers of the disease spread, leading to attack rates lower than what is expected using homogeneous assumptions [24]. Provided there is no potential for

re-infection, as was the prevailing idea during the early stages of the pandemic, it can be concluded that there is no need to allow for a larger percentage of the population to be immune (through infection) for an epidemic to end, with only 47-60% required depending on the variant transmissibility estimated for the COVID-19. Vaccinating eligible age groups in the population allows for another avenue of increasing herd immunity that does not rely on infecting the population, ending the epidemic with a lower overall attack rate. In the case where there is more than one variant of the virus present in the population, and with vaccines available, the extent to which the population is infected depends on the vaccine efficacy against these variants.

With re-infection, the interpretation of ending the COVID-19 pandemic may be modified, based on the fact that immunity generated by either prior infection or vaccination wanes over time. However, it was observed that peaks corresponding to secondary infections in all scenarios are significantly lower than those of primary infections, which means that the number of new infections generated is not as alarming due to partial immunity. This trend was also observed in the case of multiple variants, with Delta infections being lower despite being more transmissible than the Alpha variant. In this case, the "end" of the pandemic is not the complete eradication of new cases, but a steady state of new infections caused by the balancing-out of waning immunity and re-infection effects.

In this thesis, some assumptions were made in the model that would influence the results obtained. Since a deterministic model was used, the results do not account for stochasticity in disease transmission and variations in the duration of disease stages. It would prudent to extend the model and examine whether adding randomness to the system further decreases the herd immunity level required. Moreover, the community and household contact matrices used in determining the force of infection does not discriminate between unique contacts and repeated contacts. It is then possible for an individual to have repeated contacts and infect another individual, or have a higher contact rate due to interaction with different individuals

with lower rate of infection. Using an agent-based model would allow for these variations in contacts per individual to be implemented, generating an ensemble of results from possible outcomes.

This thesis involves only two doses of Moderna and Pfizer-BioNTech vaccines; as of September 2022, first and second booster shots (also referred to as third and fourth doses) have been distributed in Ontario in order to counter loss of immunity and protect against new variants such as Omicron [76]. Extending the model to include these booster doses, as well as their corresponding vaccine effectiveness [77, 78] would allow for a more accurate picture of disease dynamics in the population caused by different variants.

While this thesis has largely focused on COVID-19 pandemic, the model can be adapted to other emerging infectious diseases with similar disease characteristics, while updating disease-specific parameters. Understanding the level of herd immunity required for disease control would allow for appropriate intervention measures to be implemented in order to prevent the epidemic from progressing further and prevent re-bound.

Appendix A

Simulations with different initial conditions

In this section, the variations in simulated results caused by changing initial conditions will be illustrated. Recall that for the results obtained in this thesis, one individual with pre-symptomatic illness was introduced in each age group, with a total of seven initial infections. With the same number of total initial infections, these were introduced into simulations in different disease stages of and age groups, as presented in Table A.1.

Figure A.1 shows varying the distribution of the 7 initial infections based on age groups insignificantly changes the course of the epidemic over time, in terms of both the peak amplitude, and the peak timing. Introducing infections among children appears to cause a slightly faster epidemic growth.

Table A.1: Different initial conditions considered for simulations and comparing results.

Initial Conditions	Stage of disease	Number of initial infections per age group
IC1	Pre-symptomatic stage	1 per age group
		2 (18-49), 2 (50-64), 2 (65-79), 1 (80+)
		2 (0-4), 2 (5-11), 3 (12-17)
		7 (18-49)
IC2	Asymptomatic stage	same as IC1
IC3	Latent stage	same as IC1
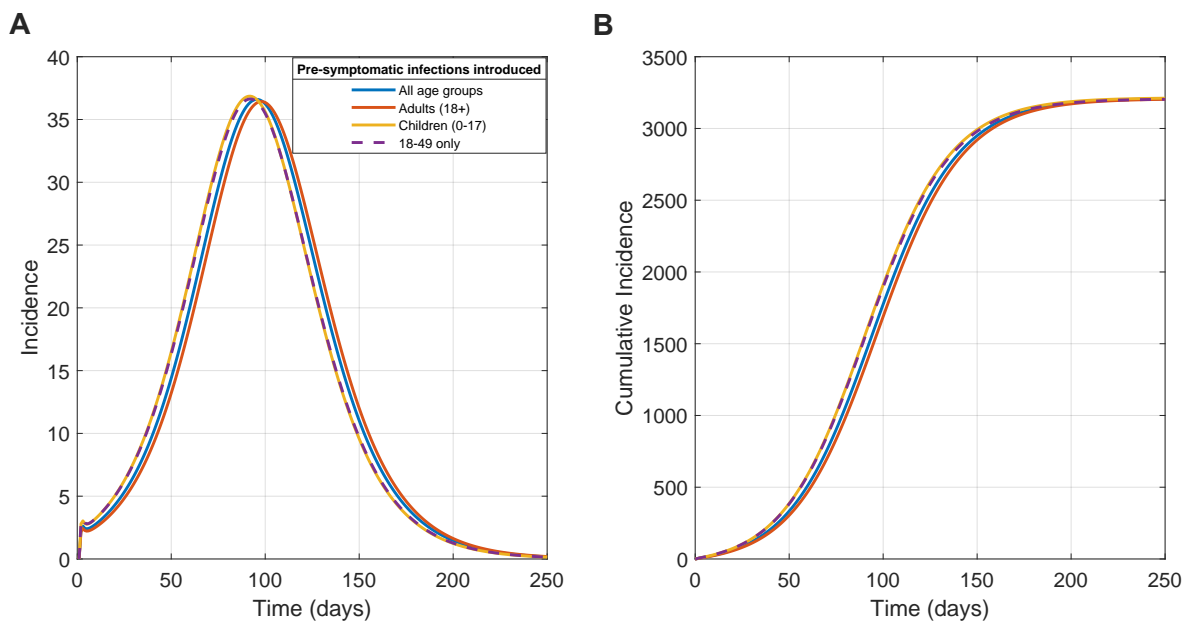
Figure A.1: Incidence (A) and cumulative incidence (B) of the original variant (S1), with 10% pre-existing immunity, no control measures, and varying initial pre-symptomatic infections (IC1).

Figure A.2: Incidence (A) and cumulative incidence (B) of the original variant (S1), with 10% pre-existing immunity, no control measures, and varying initial asymptomatic infections (IC2).

In changing the stage in which the initial infections are introduced, a more noticeable effect can be seen, especially in terms of epidemic growth rate. As shown in Figure A.2, the shift in the incidence peak is more apparent as asymptomatic individuals become the initial source of infections in the population. Within the same disease stage, varying the ages of these initial infections resulted in similar effect but less pronounced (Figure A.2). With the introduction of latent infections instead, as shown in Figure A.3, similar trends were observed, albeit with a minimal shift in incidence peak compared to the introduction of initial infections in the asymptomatic stage.
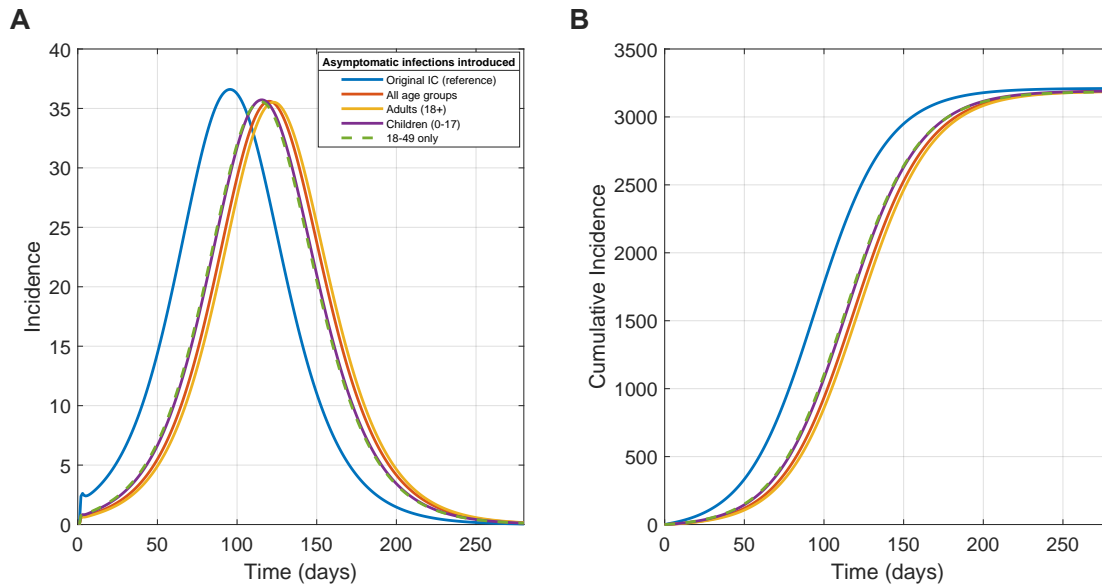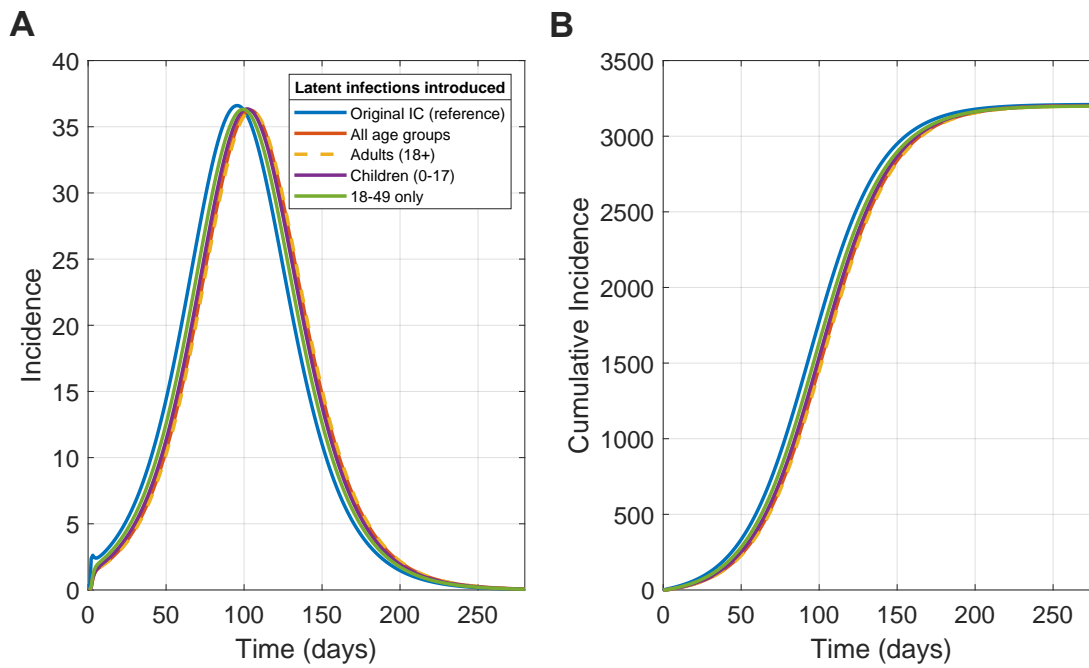
Figure A.3: Incidence (A) and cumulative incidence (B) of the original variant (S1), with 10% pre-existing immunity, no control measures, and varying initial latent infections (IC3).

Bibliography

[1] *China's first confirmed Covid-19 case traced back to November 17.* 2020. URL: `https://www.scmp.com/news/china/society/article/3074991/coronavirus-chinas-first-confirmed-covid-19-case-traced-back`.

[2] *WHO Coronavirus (COVID-19) Dashboard.* URL: `https://covid19.who.int`.

[3] Public Health Agency of Canada. *COVID-19: Outbreak update.* 2020. URL: `https://www.canada.ca/en/public-health/services/diseases/2019-novel-coronavirus-infection.html`.

[4] S. Flaxman et al. *Report 13: Estimating the number of infections and the impact of non-pharmaceutical interventions on COVID-19 in 11 European countries.* 2020. DOI: `10.25561/77731`.

[5] *Advice for the public on COVID-19 – World Health Organization.* URL: `https://www.who.int/emergencies/diseases/novel-coronavirus-2019/advice-for-public`.

[6] *Updates on COVID-19 Variants of Concern (VOC).* 2022. URL: `https://nccid.ca/covid-19-variants/`.

[7] *Tracking SARS-CoV-2 variants.* URL: `https://www.who.int/activities/tracking-SARS-CoV-2-variants`.

[8] Russell M. Viner et al. "Susceptibility to SARS-CoV-2 Infection Among Children and Adolescents Compared With Adults: A Systematic Review and Meta-analysis". In: *JAMA Pediatr* 175.2 (2021), p. 143. DOI: `10.1001/jamapediatrics.2020.4573`.

[9] Nicholas G. Davies et al. "Increased mortality in community-tested cases of SARS-CoV-2 lineage B.1.1.7". In: *Nature* 593.7858 (2021), pp. 270–274. DOI: `10.1038/s41586-021-03426-1`.

[10] Finlay Campbell et al. "Increased transmissibility and global spread of SARS-CoV-2 variants of concern as at June 2021". In: *Euro Surveill* 26.24 (2021), p. 2100509. DOI: `10.2807/1560-7917.ES.2021.26.24.2100509`.

[11] David N. Fisman and Ashleigh R. Tuite. "Evaluation of the relative virulence of novel SARS-CoV-2 variants: a retrospective cohort study in Ontario, Canada". In: *CMAJ* 193.42 (2021), E1619–E1625. DOI: `10.1503/cmaj.211248`.

[12] Neil Ferguson et al. *Report 50 - Hospitalisation risk for Omicron cases in England.* URL: `https://www.imperial.ac.uk/medicine/departments/school-public-health/infectious-disease-epidemiology/mrc-global-infectious-disease-analysis/covid-19/report-50-severity-omicron/`.

[13] Nicole Wolter et al. "Early assessment of the clinical severity of the SARS-CoV-2 omicron variant in South Africa: a data linkage study". In: *Lancet* 399.10323 (2022), pp. 437–446. DOI: `10.1016/S0140-6736(22)00017-4`.

[14] Juliet R. C. Pulliam et al. "Increased risk of SARS-CoV-2 reinfection associated with emergence of Omicron in South Africa". In: *Science* 376.6593 (2022), eabn4947. DOI: `10.1126/science.abn4947`.

[15] Jonathan Bastard et al. "Impact of the Omicron variant on SARS-CoV-2 reinfections in France, March 2021 to February 2022". In: *Euro Surveill* 27.13 (2022), p. 2200247. DOI: 10.2807/1560-7917.ES.2022.27.13.2200247.

[16] Paul Fine, Ken Eames, and David L. Heymann. ""Herd Immunity": A Rough Guide". In: *Clin Infect Dis* 52.7 (2011), pp. 911–916. DOI: 10.1093/cid/cir007.

[17] O. Diekmann and J. A. P. Heesterbeek. *Mathematical Epidemiology of Infectious Diseases: Model Building, Analysis and Interpretation*. Wiley, 2000. ISBN: 978-0-471-98682-9.

[18] Herbert W. Hethcote. "The Mathematics of Infectious Diseases". In: *SIAM Rev.* 42.4 (2000), pp. 599–653. DOI: 10.1137/S0036144500371907.

[19] Roy M. Anderson and Robert M. May. *Infectious Diseases of Humans: Dynamics and Control*. OUP Oxford, 1992. ISBN: 978-0-19-854040-3.

[20] Matt J. Keeling and Pejman Rohani. *Modeling Infectious Diseases in Humans and Animals*. Princeton University Press, 2011. ISBN: 978-1-4008-4103-5.

[21] Almut Scherer and Angela McLean. "Mathematical models of vaccination". In: *Br Med Bull* 62.1 (2002), pp. 187–199. DOI: 10.1093/bmb/62.1.187.

[22] Fan Bai. "Vaccination models in infectious diseases". PhD thesis. University of British Columbia, 2016. DOI: 10.14288/1.0305652.

[23] Zhen Wang et al. "Statistical physics of vaccination". In: *Physics Reports* 664 (2016), pp. 1–113. DOI: 10.1016/j.physrep.2016.10.006.

[24] Tom Britton, Frank Ball, and Pieter Trapman. "A mathematical model reveals the influence of population heterogeneity on herd immunity to SARS-CoV-2". In: *Science* 369.6505 (2020), pp. 846–849. DOI: 10.1126/science.abc6810.

[25] Tobias S. Brett and Pejman Rohani. "Transmission dynamics reveal the impracticality of COVID-19 herd immunity strategies". In: *Proceedings of the National Academy of Sciences* 117.41 (2020), pp. 25897–25903. DOI: `10.1073/pnas.2008087117`.

[26] Andrew A. Sayampanathan et al. "Infectivity of asymptomatic versus symptomatic COVID-19". In: *Lancet* 397.10269 (2021), pp. 93–94. DOI: `10.1016/S0140-6736(20) 32651-9`.

[27] Luca Ferretti et al. "Quantifying SARS-CoV-2 transmission suggests epidemic control with digital contact tracing". In: *Science* 368.6491 (2020), eabb6936. DOI: `10.1126/ science.abb6936`.

[28] Xi He et al. "Temporal dynamics in viral shedding and transmissibility of COVID-19". In: *Nat Med* 26.5 (2020), pp. 672–675. DOI: `10.1038/s41591-020-0869-5`.

[29] Seyed M. Moghadas et al. "Projecting hospital utilization during the COVID-19 outbreaks in the United States". In: *Proc Natl Acad Sci U S A* 117.16 (2020), pp. 9122–9126. DOI: `10.1073/pnas.2004064117`.

[30] *Ontario Confirms First Case of Wuhan Novel Coronavirus*. URL: `https://news. ontario.ca/en/release/55486/ontario-confirms-first-case-of-wuhan-novel- coronavirus`.

[31] *Death in Ontario Potentially Related to COVID-19*. en. URL: `https://news.ontario. ca/en/statement/56358/death-in-ontario-potentially-related-to-covid-19`.

[32] *Ontario Enacts Declaration of Emergency to Protect the Public*. URL: `https://news. ontario.ca/en/release/56356/ontario-enacts-declaration-of-emergency-to- protect-the-public`.

[33] *Coronavirus: Bobcaygeon nursing home 'closer to putting outbreak behind' them.* URL: https://globalnews.ca/news/6853802/coronavirus-bobcaygeon-nursing-home-stable/.

[34] Ontario Agency for Health Protection and Promotion (Public Health Ontario). *Enhanced Epidemiological Summary: COVID-19 in Long-Term Care Homes in Ontario: January 15, 2020 to February 28, 2021.* 2021. URL: https://www.publichealthontario.ca/-/media/documents/ncov/epi/2020/06/covid-19-epi-ltch-residents.pdf?la=en.

[35] *Ontario sees single-day record of 700 new COVID-19 cases as calls grow to return to Stage 2.* 2020. URL: https://www.cbc.ca/news/canada/toronto/covid-19-coronavirus-ontario-numbers-september-28-1.5741454.

[36] *Ontario's 2nd wave of COVID-19 forecast to peak in October.* 2020. URL: https://www.cbc.ca/news/canada/toronto/ontario-covid-19-second-wave-cases-modelling-projections-1.5739411.

[37] *Ontario Confirms First Cases of COVID-19 UK Variant in Ontario.* URL: https://news.ontario.ca/en/release/59831/ontario-confirms-first-cases-of-covid-19-uk-variant-in-ontario.

[38] *Ontario confirms first case of South African COVID-19 variant.* URL: https://www.theglobeandmail.com/canada/article-covid-19-in-ontario-province-reports-1969-new-cases-36-additional/.

[39] Ontario Agency for Health Protection and Promotion (Public Health Ontario). *Enhanced epidemiological summary: COVID-19 variants of concern in Ontario: December 1, 2020 to March 28, 2021.* URL: https://www.publichealthontario.ca/-/media/documents/ncov/epi/covid-19-variant-epi-summary.pdf?la=en.

[40] *'Our situation is dire,' top health official says as Ontario sees 4,736 new COVID-19 cases | CBC News.* 2021. URL: https://www.cbc.ca/news/canada/toronto/covid-19-ontario-april-15-2021-new-cases-1.5988571.

[41] *Ontario marks lowest COVID-19 daily case count in months.* 2021. URL: https://toronto.ctvnews.ca/ontario-marks-lowest-covid-19-daily-case-count-in-months-1.5621279.

[42] Ontario Agency for Health Protection and Promotion (Public Health Ontario). *Estimating the Prevalence and Growth of SARS-CoV-2 Variants in Ontario using Mutation Profiles.* URL: https://www.publichealthontario.ca/-/media/documents/ncov/epi/covid-19-prevalence-growth-voc-mutation-epi-summary.pdf?sc_lang=en.

[43] *Ontario reports first two cases of Omicron COVID-19 variant.* 2021. URL: https://toronto.ctvnews.ca/ontario-reports-first-two-cases-of-omicron-covid-19-variant-1.5684897.

[44] *Early Dynamics of Omicron in Ontario, November 1 to December 9, 2021.* 2021. URL: https://www.publichealthontario.ca/-/media/documents/ncov/epi/covid-19-early-dynamics-omicron-ontario-epi-summary.pdf.

[45] *COVID-19 in Ontario: January 15, 2020 to December 31, 2021.* 2020. URL: https://files.ontario.ca/moh-covid-19-report-en-2022-01-01.pdf.

[46] *The BA.5 subvariant is fuelling another COVID wave.* 2022. URL: https://www.cbc.ca/news/health/covid-wave-ba5-ba4-subvariant-1.6513639.

[47] *Ontario's COVID-19 vaccination plan.* URL: https://covid-19.ontario.ca/ontarios-covid-19-vaccination-plan.

[48] Public Health Agency of Canada. *Archive 22: Recommendations on the use of COVID-19 vaccines [2021-10-22]*. URL: https://www.canada.ca/en/public-health/services/immunization/national-advisory-committee-on-immunization-naci/recommendations-use-covid-19-vaccines.html.

[49] *Ontario unveils details of AstraZeneca COVID-19 vaccine pharmacy pilot*. 2021. URL: https://www.cbc.ca/news/canada/toronto/covid-19-ontario-march-10-2021-astrazeneca-pharmacies-1.5943618.

[50] *Setting Ontario's vaccination priorities*. URL: https://covid-19.ontario.ca/setting-ontarios-vaccination-priorities.

[51] *Ontario Prepares to Accelerate Rollout as Vaccine Supply Increases*. URL: https://news.ontario.ca/en/release/1000035/ontario-prepares-to-accelerate-rollout-as-vaccine-supply-increases.

[52] *AstraZeneca's COVID-19 vaccine: EMA finds possible link to very rare cases of unusual blood clots with low platelets*. 2021. URL: https://www.ema.europa.eu/en/news/astrazenecas-covid-19-vaccine-ema-finds-possible-link-very-rare-cases-unusual-blood-clots-low-blood.

[53] Benjamin Chan et al. "Risk of Vaccine-Induced Thrombotic Thrombocytopenia (VITT) following the AstraZeneca/COVISHIELD Adenovirus Vector COVID-19 Vaccines". In: *Science Briefs of the Ontario COVID-19 Science Advisory Table* 2.28 (2021). DOI: 10.47326/ocsat.2021.02.28.1.0.

[54] Public Health Agency of Canada. *Archived 8: AstraZeneca COVID-19 vaccine use in younger adults: NACI recommendation*. 2021. URL: https://www.canada.ca/en/public-health/services/immunization/national-advisory-committee-on-immunization-naci/rapid-response-recommended-use-astrazeneca-covid-19-vaccine-younger-adults.html.

[55] Ontario Agency for Health Protection and Promotion (Public Health Ontario). *COVID-19 viral vector vaccines and rare blood clots – vaccine safety surveillance in action.* 2021. URL: `https://www.publichealthontario.ca/-/media/Documents/nCoV/Vaccines/2021/07/covid-19-viral-vector-vaccines-rare-blood-clots.pdf?sc_lang=en`.

[56] *Ontario will no longer give AstraZeneca COVID-19 vaccine as 1st dose due to blood clot risk.* 2021. URL: `https://www.cbc.ca/news/canada/toronto/ontario-update-astrazeneca-vaccine-1.6022545`.

[57] Public Health Agency of Canada. *COVID-19 vaccine extended dose intervals for early vaccine rollout and population protection in Canada: NACI recommendations.* 2021. URL: `https://www.canada.ca/en/public-health/services/immunization/national-advisory-committee-on-immunization-naci/extended-dose-intervals-covid-19-vaccines-early-rollout-population-protection.html`.

[58] *Accelerated Second Dose Eligibility Continues Ahead of Schedule.* URL: `https://news.ontario.ca/en/release/1000367/accelerated-second-dose-eligibility-continues-ahead-of-schedule`.

[59] Elie Dolgin. "COVID vaccine immunity is waning — how much does that matter?" In: *Nature* 597.7878 (2021), pp. 606–607. DOI: `10.1038/d41586-021-02532-4`.

[60] Yair Goldberg et al. "Waning Immunity after the BNT162b2 Vaccine in Israel". In: *N Engl J Med* 385.24 (2021), e85. DOI: `10.1056/NEJMoa2114228`.

[61] *Ontario Expanding Booster Eligibility to More Ontarians.* URL: `https://news.ontario.ca/en/release/1001100/ontario-expanding-booster-eligibility-to-more-ontarians`.

[62] *All Ontarians 18+ Eligible for COVID-19 Booster Appointments at Three-Month Interval.* URL: `https://news.ontario.ca/en/release/1001352/all-ontarians-18-eligible-for-covid-19-booster-appointments-at-three-month-interval`.

[63] Katia J. Bruxvoort et al. "Effectiveness of mRNA-1273 against delta, mu, and other emerging variants of SARS-CoV-2: test negative case-control study". In: *BMJ* 375 (2021), e068848. DOI: `10.1136/bmj-2021-068848`.

[64] Sharifa Nasreen et al. "Effectiveness of COVID-19 vaccines against symptomatic SARS-CoV-2 infection and severe outcomes with variants of concern in Ontario". In: *Nat Microbiol* 7.3 (2022), pp. 379–385. DOI: `10.1038/s41564-021-01053-0`.

[65] Noa Dagan et al. "BNT162b2 mRNA Covid-19 Vaccine in a Nationwide Mass Vaccination Setting". In: *N Engl J Med* 384.15 (2021), pp. 1412–1423. DOI: `10.1056/NEJMoa2101765`.

[66] Laith J. Abu-Raddad, Hiam Chemaitelly, and Adeel A. Butt. "Effectiveness of the BNT162b2 Covid-19 Vaccine against the B.1.1.7 and B.1.351 Variants". In: *N Engl J Med* (2021), NEJMc2104974. DOI: `10.1056/NEJMc2104974`.

[67] Koen B. Pouwels et al. "Effect of Delta variant on viral burden and vaccine effectiveness against new SARS-CoV-2 infections in the UK". In: *Nat Med* 27.12 (2021), pp. 2127–2135. DOI: `10.1038/s41591-021-01548-7`.

[68] Qun Li et al. "Early Transmission Dynamics in Wuhan, China, of Novel Coronavirus–Infected Pneumonia". In: *N Engl J Med* 382.13 (2020), pp. 1199–1207. DOI: `10.1056/NEJMoa2001316`.

[69] Seyed M. Moghadas et al. "The implications of silent transmission for the control of COVID-19 outbreaks". In: *Proc Natl Acad Sci U S A* 117.30 (2020), pp. 17513–17515. DOI: `10.1073/pnas.2008373117`.

[70] Ruiyun Li et al. "Substantial undocumented infection facilitates the rapid dissemination of novel coronavirus (SARS-CoV-2)". In: *Science* 368.6490 (2020), pp. 489–493. DOI: `10.1126/science.abb3221`.

[71] Steven Sanche et al. "High Contagiousness and Rapid Spread of Severe Acute Respiratory Syndrome Coronavirus 2". In: *Emerg Infect Dis* 26.7 (2020), pp. 1470–1477. DOI: `10.3201/eid2607.200282`.

[72] Seyed M. Moghadas et al. "Simulated Identification of Silent COVID-19 Infections Among Children and Estimated Future Infection Rates With Vaccination". In: *JAMA Netw Open* 4.4 (2021), e217097. DOI: `10.1001/jamanetworkopen.2021.7097`.

[73] Joël Mossong et al. "Social Contacts and Mixing Patterns Relevant to the Spread of Infectious Diseases". In: *PLOS Medicine* 5.3 (2008), e74. DOI: `10.1371/journal.pmed.0050074`.

[74] Christopher I. Jarvis et al. "Quantifying the impact of physical distance measures on the transmission of COVID-19 in the UK". In: *BMC Medicine* 18.1 (2020), p. 124. DOI: `10.1186/s12916-020-01597-8`.

[75] Seyed M. Moghadas. *Mathematical Modelling: A Graduate Textbook*. Hoboken: John Wiley and Sons, 2019.

[76] *Getting the COVID-19 vaccine.* URL: `https://covid-19.ontario.ca/getting-covid-19-vaccine`.

[77] Stijn P. Andeweg et al. "Protection of COVID-19 vaccination and previous infection against Omicron BA.1, BA.2 and Delta SARS-CoV-2 infections". In: *Nat Commun* 13.1 (2022), p. 4738. DOI: `10.1038/s41467-022-31838-8`.

[78]   Mark G. Thompson. "Effectiveness of a Third Dose of mRNA Vaccines Against COVID-19–Associated Emergency Department and Urgent Care Encounters and Hospitalizations Among Adults During Periods of Delta and Omicron Variant Predominance — VISION Network, 10 States, August 2021–January 2022". In: *MMWR Morb Mortal Wkly Rep* 71.4 (2022). DOI: `10.15585/mmwr.mm7104e3`.